IEEE Access
Multidisciplinary ⋮ Rapid Review ⋮ Open Access Journal

Received September 16, 2019, accepted October 16, 2019, date of publication October 24, 2019, date of current version November 8, 2019.

Digital Object Identifier 10.1109/ACCESS.2019.2949372

A Loop-Analysis Theory Based Linear Power Flow Method for Three-Phase Distribution Power System

HONGWEI LI[1,2], HAILIN ZHOU[1], TONG LIU[1], AND QI CHEN[1]

[1]School of Electrical Engineering and Information, Southwest Petroleum University, Chengdu 610500, China
[2]Energy Equipment Institute, Southwest Petroleum University, Chengdu 610500, China

Corresponding author: Hongwei Li (lhw@swpu.edu.cn)

This work was supported in part by the Chinese National Key Basic Research and Development Program under Grant 2013CB228203, and in part by the National Key Research and Development Project under Grant 2017YFE0112600.

ABSTRACT The linear power flow (LPF) models are particularly important in the context of optimization algorithms for three-phase distribution systems with the high penetration of distributed renewable generations. With several approximations on network modelling, voltage drop calculation, link power calculation, voltage controlled bus and ZIP loads, this paper proposed a three-phase LPF model for three-phase unbalanced distribution networks based on loop-analysis theory. The method can deal with voltage-controlled (PV) & Load (PQ) buses and ZIP loads. The approximations of the star and delta connections ZIP loads are also analyzed. Test results based on several standard IEEE test feeders and an improved 615bus test system proved the effectiveness and accuracy of the proposed algorithm. The proposed LPF solution gives a simple, more robust, and potentially faster solution for modern distribution power system.

INDEX TERMS Linear power flow (LPF), unbalanced distribution network, three-phase ZIP load, link branch power, linear approximation.

LIST OF SYMBOLS

$\vec{V}$ means a diagonal matrix by putting the vector $\boldsymbol{V}$ on the main diagonal of a square matrix.

$\alpha = \exp(\mathrm{j}2\pi/3)$ and $\boldsymbol{\Phi} = \mathrm{diag}([1, \alpha^2, \alpha])$.

$\mathbf{R} + \mathrm{j}\mathbf{X}$ are the coupled line parameters for a branch

$\hat{\mathbf{R}} + \mathrm{j}\hat{\mathbf{X}}$ are the modified coupled line parameters for a branch, $\hat{\mathbf{R}} + \mathrm{j}\hat{\mathbf{X}} = \boldsymbol{\Phi}^{-1}(\mathbf{R} + \mathrm{j}\mathbf{X})\boldsymbol{\Phi}$.

$\boldsymbol{U}_\mathrm{i} = [U_\mathrm{ia}; U_\mathrm{ib}; U_\mathrm{ic}]$ and $\boldsymbol{\theta}_\mathrm{i} = [\theta_\mathrm{ia}; \theta_\mathrm{ib}; \theta_\mathrm{ic}]$ are the three-phase voltage magnitude and phase angle vectors for bus i.

$\mathrm{d}\boldsymbol{U} = [\mathrm{d}U_\mathrm{a}; \mathrm{d}U_\mathrm{b}; \mathrm{d}U_\mathrm{c}]$ and $\mathrm{d}\hat{\boldsymbol{\theta}} = [\hat{\theta}_\mathrm{a}; \hat{\theta}_\mathrm{b}; \hat{\theta}_\mathrm{c}]$is the three-phase voltage drop and angle difference vectors along a branch.

$\boldsymbol{P}_\mathrm{o} = [P_\mathrm{oa}; P_\mathrm{ob}; P_\mathrm{oc}]$ and $\boldsymbol{Q}_\mathrm{o} = [Q_\mathrm{oa}; Q_\mathrm{ob}; Q_\mathrm{oc}]$ are the three-phase active and reactive power (load) vectors.

$\mathrm{d}\boldsymbol{P} = [\mathrm{d}P_\mathrm{a}; \mathrm{d}P_\mathrm{b}; \mathrm{d}P_\mathrm{c}]$ and $\mathrm{d}\boldsymbol{Q} = [\mathrm{d}Q_\mathrm{a}; \mathrm{d}Q_\mathrm{b}; \mathrm{d}Q_\mathrm{c}]$ are the three-phase active and reactive power loss vectors along a branch.

$\boldsymbol{P}_\mathrm{L} = [P_\mathrm{ab}; P_\mathrm{bc}; P_\mathrm{ca}]$ and $\boldsymbol{Q}_\mathrm{L} = [\boldsymbol{Q}_\mathrm{ab}; Q_\mathrm{bc}; Q_\mathrm{ca}]$ are the line load vector, the star load vector,

$\hat{\boldsymbol{P}} = [\hat{P}_\mathrm{a}; \hat{P}_\mathrm{b}; \hat{P}_\mathrm{c}]$ and $\hat{\boldsymbol{Q}} = [\hat{Q}_\mathrm{a}; \hat{Q}_\mathrm{b}; \hat{Q}_\mathrm{c}]$ are the equivalent phase-ground load vectors corresponding to the delta connection load.

$\boldsymbol{P}_{j\Sigma} = [P_{j\sum\mathrm{a}}; P_{j\sum\mathrm{b}}; P_{j\sum\mathrm{c}}]$ and $\boldsymbol{Q}_{j\Sigma} = [Q_{j\sum\mathrm{a}}; Q_{j\sum\mathrm{b}}; Q_{j\sum\mathrm{c}}]$ are the equivalent phase-ground **IP** type load vectors corresponding to the hybrid star and delta connection **ZIP** loads.

$\mathbf{T}_\mathrm{t}$ is the 3N*3N path matrix corresponding to tree branches for DPS.

$\mathbf{B}_\mathrm{t}$ is the 3m*3N loop matrix corresponding to tree branches for DPS.

$\boldsymbol{U}_\mathrm{n} = [\boldsymbol{U}_1; \boldsymbol{U}_2; \cdots; \boldsymbol{U}_\mathrm{N}]$ and $\boldsymbol{\theta}_\mathrm{n} = [\boldsymbol{\theta}_1; \boldsymbol{\theta}; \cdots; \boldsymbol{\theta}_\mathrm{N}]$ are the bus voltage magnitude and angle vectors.

$\mathrm{d}\boldsymbol{U}_\mathrm{t} = [\mathrm{d}\boldsymbol{U}_1; \mathrm{d}\boldsymbol{U}_2; \cdots; \mathrm{d}\boldsymbol{U}_\mathrm{N}]$ and $\mathrm{d}\boldsymbol{\theta}_\mathrm{t} = [\mathrm{d}\boldsymbol{\theta}_1; \mathrm{d}\boldsymbol{\theta}_2; \cdots; \mathrm{d}\boldsymbol{\theta}_\mathrm{N}]$ are the branch drop and angle difference vectors.

$\boldsymbol{Q}_\mathrm{I} = [\boldsymbol{Q}_\mathrm{It}; \boldsymbol{Q}_{Il}] = [\boldsymbol{Q}_{\mathrm{i}1}; \boldsymbol{Q}_{\mathrm{i}2}; \cdots; \boldsymbol{Q}_{\mathrm{i}(\mathrm{N}+\mathrm{m})}]$ and $\boldsymbol{P}_\mathrm{I} = [\boldsymbol{P}_\mathrm{It}; \boldsymbol{P}_{Il}] = [\boldsymbol{P}_{\mathrm{i}1}; \boldsymbol{P}_{\mathrm{i}2}; \cdots; \boldsymbol{P}_{\mathrm{i}(\mathrm{N}+\mathrm{m})}]$ are the branch reactive and active power vectors.

$\boldsymbol{P} = [\boldsymbol{P}_1; \boldsymbol{P}_2; \cdots; \boldsymbol{P}_\mathrm{N}]$ and $\boldsymbol{Q} = [\boldsymbol{Q}_1; \boldsymbol{Q}_2; \cdots; \boldsymbol{Q}_\mathrm{N}]$ are the bus consumption active and reactive power vectors for **P** type load.

The associate editor coordinating the review of this manuscript and approving it for publication was Ahmed F. Zobaa.

$\boldsymbol{P}_{P\Sigma} = [\boldsymbol{P}_{1P\Sigma}; \boldsymbol{P}_{2P\sum}; \cdots; \boldsymbol{P}_{NP\sum}]$ and $\boldsymbol{Q}_{P\Sigma} = [\boldsymbol{Q}_{1P\Sigma}; \boldsymbol{Q}_{2P\sum}; \cdots; \boldsymbol{Q}_{NP\sum}]$ are the bus consumption active and reactive power vectors for ZIP type load.

I. INTRODUCTION

Robust power flow is very important for modern distribution power system (DPS) management, especially with the high penetration of distributed renewable generation into the traditional distribution networks. Because of the unbalance and high R/X features of DPS, the conventional iterative power flow methods are limited in speed and reliability for real-time optimization and control [1]. In order to deal with the nonlinear optimization problems of DPS, the non-iterative and direct calculation of power flow, that is, the linear power flow (LPF) solutions show many advantages and had been studied by many researchers. Based on LPFs, the optimization problems of DPS can be formulated and solved more efficiently. The LPFs with the reasonable accuracy and robustness have been applied to the ordered charging of electric vehicle [2], [3], probabilistic load flow [4], [5], Volt-VAR Optimization [6], and network reconfiguration [7] etc..

Traditional DC power flow (DCPF) model has been widely used as a LPF method. However, DCPF is limited with the assumptions of the lossless branch power flows and the flat bus voltage magnitudes [1]. But the voltage limits and reactive load flows are vital constraints in the actual distribution power systems and thus, cannot be omitted. Moreover, DCPF cannot be directly applied in DPS due to the high R/X features of DPS.

Three parts are important for LPF solutions in DPS. That is, the model should be capable of applying to weakly meshed three-phase unbalanced systems, can deal with the widely used ZIP type load (consisting of a constant impedance, Z, a constant current, I, and a constant power, P) and can deal with the voltage-controlled (PV) buses.

Most LPFs are developed under rectangular coordinates. In [8], a linear approximation of power flow has been proposed in multiphase radial network with semidefinite relaxation formulation. In [9], as an extension of [8], it presented a group of relatively simple LPF approximation equations for radial three-phase network, but the voltage angles were omitted. Moreover, the methods in [8], [9] cannot deal with ZIP load and PV bus. In [10], a ZIP linearization model has been developed from the complex field with the approximation $1/\dot{U} \approx 2 - \dot{U}^*$ (superscript '*' indicates complex conjugate). And in [11], based on the curve-fitting technique, a voltage-dependent load model was derived by splitting the ZIP load as a combination of an impedance source and a current source. In [12], a three-phase linear power flow formulation has been derived based on the fact that voltage angles and magnitudes vary within relatively narrow boundaries. ZIP loads have been approximated based on a curve-fitting technique. In [13], a loop-analysis theory based LPF solution has been proposed for balanced and unbalanced systems. The ZIP loads have been handled similarly as in [10]. However, all those methods in [8]–[13] have been developed under rectangular coordinates and cannot deal with the PV buses. The voltages in those methods were decomposed into the real and imaginary parts as $\dot{U} = U\angle\theta = U_{re} + jU_{im}$ (the subscripts 're' and 'im' denote real and imagine part of voltage), so the assumptions that the bus voltage magnitude $U \approx 1.0$p.u. and branch voltage angle difference $\theta_{ij} \approx 0$ cannot be directly used under rectangular coordinates. Thus, those LPF methods cannot cope with the PV buses easily and directly.

In order to deal with PV buses, LPFs under the polar coordinates are frequently emphasized. In [14], [15], with $\cos\theta_{ij} \approx 1$, $\sin\theta_{ij} \approx \theta_{ij}$ and by selectively setting $U_i \approx 1.0$, two similar LPF methods have been developed under polar coordinates for balanced distribution system but PV buses and ZIP loads were not discussed. In [16], based on the logarithmic transform of voltage magnitudes and the approximation analysis of the general branch flows, a LPF model including PV and PQ buses and tap changers was proposed for the balanced distribution power system. In [17], based on LPF equations as in [14], an improved decoupled single-phase linear power flow (DLPF) model has been proposed with considering PV buses. In [18], a linear three-phase power flow model has been proposed for an active distribution network with the consideration of the ZIP type of the loads and PV buses. In [19], it derived a general three-phase LPF model under the polar coordinates. The method can account for ZIP loads, transformers and DGs, but the method is relatively complicated.

Considering the different network features and the different application requirements, the LPF needs to be further studied. On the basis of the past work, that is, a loop-analysis theory based single-phase linear power flow methods in [20], and considering the approximate balance of three-phase DPS, this paper proposed a three-phase LPF model for three-phase unbalanced distribution network considering PV & PQ buses and ZIP load. The proposed model is distinguished from above methods by its formation with loop-analysis theory based power flows calculation under polar coordinates. The proposed LPF has enough accuracy in voltage magnitude and has higher computational efficiency because the calculation matrix dimension is half of the dimension of other calculation matrixes in [11]–[13], [18], [19].

The rest of this paper is organized as follows. Section 2 introduces the linearization and approximation of network model and ZIP load. Section 3 proposes the approximate calculations of link powers and PV buses and then presents the three-phase unbalanced LPF solution. Section 4 is the numerical tests based on some IEEE test systems. Section 5 concludes the work.

II. LINEARIZATION OF NETWORK MODELLING AND ZIP LOAD

In this section, considering that the angles of the three-phase voltages at the same bus are nearly symmetrical, several linear approximations have been developed for a three-phase unbalanced system. The approximate calculations include

the three-phase voltage drop and angle difference along one branch, the three-phase ZIP load to three-phase IP load conversion and the output reactive power of the shunt **B.**

Considering that the distribution lines are not very long, a typical three-phase distribution line can be modeled as a π elements as shown in Figure 1 (in the electrical parameters, the shunt conductance parameters are ignored). Unlike the balanced system which is discussed in [20]–[22], the three-phase line parameters in a three-phase unbalanced system are coupled and unbalanced as well as the unbalanced loads. Thus, the power flow method needs to be redeveloped.

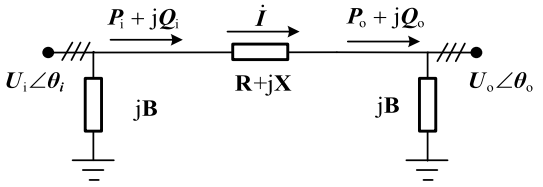

FIGURE 1. The equivalent π circuit of three-phase distribution branches.

A. APPROXIMATION OF VOLTAGE DROP AND ANGLE DIFFERENCE

In Fig.1, let $\boldsymbol{U}_i = [U_{ia}; U_{ib}; U_{ic}]$ and $\boldsymbol{\theta} = [\theta_{ia}; \theta_{ib}; \theta_{ic}]$, $\boldsymbol{U}_o = [U_{oa}; U_{ob}; U_{oc}]$ and $\boldsymbol{\theta}_o = [\theta_{oa}; \theta_{ob}; \theta_{oc}]$ be the three-phase voltage magnitudes (in per unit) and phase angles (in radian) for bus i and bus o respectively; let $\boldsymbol{P}_o = [P_{oa}; P_{ob}; P_{oc}]$ and $\boldsymbol{Q}_o = [Q_{oa}; Q_{ob}; Q_{oc}]$ be the three-phase active and reactive powers flowing along the branch as shown in figure 1; and the coupled line parameters can be expressed as,

$$\mathbf{R} + \mathrm{j}\mathbf{X} = \begin{bmatrix} \mathrm{R_{aa}}, \mathrm{R_{ab}}, \mathrm{R_{ac}} \\ \mathrm{R_{ba}}, \mathrm{R_{bb}}, \mathrm{R_{bc}} \\ \mathrm{R_{ca}}, \mathrm{R_{cb}}, \mathrm{R_{cc}} \end{bmatrix} + \mathrm{j}\begin{bmatrix} \mathrm{X_{aa}}, \mathrm{X_{ab}}, \mathrm{X_{ac}} \\ \mathrm{X_{ba}}, \mathrm{X_{bb}}, \mathrm{X_{bc}} \\ \mathrm{X_{ca}}, \mathrm{X_{cb}}, \mathrm{X_{cc}} \end{bmatrix} \quad (1)$$

$$\mathbf{B} = \begin{bmatrix} \mathrm{B_{aa}}, \mathrm{B_{ab}}, \mathrm{B_{ac}} \\ \mathrm{B_{ba}}, \mathrm{B_{bb}}, \mathrm{B_{bc}} \\ \mathrm{B_{ca}}, \mathrm{B_{cb}}, \mathrm{B_{cc}} \end{bmatrix} \quad (2)$$

And it has (herein, the shunt **B** can be treated as the constant susceptance load and will be discussed below),

$$\begin{bmatrix} \dot{U}_{ia} \\ \dot{U}_{ib} \\ \dot{U}_{ic} \end{bmatrix} = \begin{bmatrix} \dot{U}_{oa} \\ \dot{U}_{ob} \\ \dot{U}_{oc} \end{bmatrix} + (\mathbf{R} + \mathrm{j}\mathbf{X}) \begin{bmatrix} (P_{oa} + \mathrm{j}Q_{oa}/\dot{U}_{oa})^* \\ (P_{ob} + \mathrm{j}Q_{ob}/\dot{U}_{ob})^* \\ (P_{oc} + \mathrm{j}Q_{oc}/\dot{U}_{oc})^* \end{bmatrix} \quad (3)$$

Note that all electrical parameter are in per unit in this paper.

Let A-phase be the reference phase, for simplification, let $\alpha = \exp(\mathrm{j}2\pi/3)$, $\theta_{oa} = 0$ and $\dot{U}_{oa} = U_{oa}\angle 0$, so $\mathrm{d}\theta_a = \theta_{ia} - \theta_{oa} = \theta_{ia}$ and $\dot{U}_{ia} = U_{ia}\angle\mathrm{d}\theta_a$. Considering that the three-phase voltage angles at the same bus are almost symmetrical, that is, it has $\dot{U}_{ob} \approx \alpha^2 U_{ob}$ and $\dot{U}_{oc} \approx \alpha U_{oc}$. Define $\mathrm{d}\theta_b \approx \theta_{ib} - \theta_{ob}$ and $\mathrm{d}\theta_c \approx \theta_{ic} - \theta_{oc}$, then $\dot{U}_{ib} \approx \alpha^2 U_{ib}\angle\mathrm{d}\theta_b$ and $\dot{U}_{ic} \approx \alpha U_{ic}\angle\mathrm{d}\theta_c$. For the distribution line is not long, θ_a, θ_b and θ_c are very small and close to zero. Thus, define $\vec{\boldsymbol{P}}_o = \mathrm{diag}(\boldsymbol{P}_o)$ and $\vec{\boldsymbol{Q}}_o = \mathrm{diag}(\boldsymbol{Q}_o)$, $\boldsymbol{\Phi} = \mathrm{diag}([1, \alpha^2, \alpha])$, then (3) can be rewritten as,

$$\begin{aligned} \begin{bmatrix} \dot{U}_{ia} \\ \dot{U}_{ib} \\ \dot{U}_{ic} \end{bmatrix} &\approx \boldsymbol{\Phi} \begin{bmatrix} U_{ia}\angle\mathrm{d}\theta_a \\ U_{ib}\angle\mathrm{d}\theta_b \\ U_{ic}\angle\mathrm{d}\theta_c \end{bmatrix} \approx \boldsymbol{\Phi} \begin{bmatrix} U_{oa} \\ U_{ob} \\ U_{oc} \end{bmatrix} \\ &\quad + (\mathbf{R} + \mathrm{j}\mathbf{X})\boldsymbol{\Phi} \begin{bmatrix} (P_{oa} - \mathrm{j}Q_{oa})/U_{oa} \\ (P_{ob} - \mathrm{j}Q_{ob})/U_{ob} \\ (P_{oc} - \mathrm{j}Q_{oc})/U_{oc} \end{bmatrix} \\ &= \boldsymbol{\Phi} \begin{bmatrix} U_{oa} \\ U_{ob} \\ U_{oc} \end{bmatrix} + (\mathbf{R} + \mathrm{j}\mathbf{X})\boldsymbol{\Phi}(\vec{\boldsymbol{P}}_o - \mathrm{j}\vec{\boldsymbol{Q}}_o) \begin{bmatrix} 1/U_{oa} \\ 1/U_{ob} \\ 1/U_{oc} \end{bmatrix} \end{aligned} \quad (4)$$

By multiplying $\boldsymbol{\Phi}^{-1}$ on both sides of (4), the following equations can be deduced as,

$$\begin{bmatrix} U_{ia}\angle\mathrm{d}\theta_a \\ U_{ib}\angle\mathrm{d}\theta_b \\ U_{ic}\angle\mathrm{d}\theta_c \end{bmatrix} - \begin{bmatrix} U_{oa} \\ U_{ob} \\ U_{oc} \end{bmatrix} = \boldsymbol{\Phi}^{-1}(\mathbf{R} + \mathrm{j}\mathbf{X})\boldsymbol{\Phi}(\vec{\boldsymbol{P}}_o - \mathrm{j}\vec{\boldsymbol{Q}}_o) \begin{bmatrix} 1/U_{oa} \\ 1/U_{ob} \\ 1/U_{oc} \end{bmatrix} \quad (5)$$

Define,

$$\begin{aligned} &\hat{\mathbf{R}} + \mathrm{j}\hat{\mathbf{X}} \\ &= \boldsymbol{\Phi}^{-1}(\mathbf{R} + \mathrm{j}\mathbf{X})\boldsymbol{\Phi} \\ &= \frac{1}{2}\begin{bmatrix} 2\mathrm{R_{aa}} & \sqrt{3}\mathrm{X_{ab}} - \mathrm{R_{ab}} & -\sqrt{3}\mathrm{X_{ac}} - \mathrm{R_{ac}} \\ -\sqrt{3}\mathrm{X_{ba}} - \mathrm{R_{ba}} & 2\mathrm{R_{bb}} & \sqrt{3}\mathrm{X_{bc}} - \mathrm{R_{bc}} \\ \sqrt{3}\mathrm{X_{ca}} - \mathrm{R_{ca}} & -\sqrt{3}\mathrm{X_{cb}} - \mathrm{R_{cb}} & 2\mathrm{R_{cc}} \end{bmatrix} \\ &\quad + \frac{\mathrm{j}}{2}\begin{bmatrix} 2\mathrm{X_{aa}} & -\sqrt{3}\mathrm{R_{ab}} - \mathrm{X_{ab}} & \sqrt{3}\mathrm{R_{ac}} - \mathrm{X_{ac}} \\ \sqrt{3}\mathrm{R_{ba}} - \mathrm{X_{ba}} & 2\mathrm{X_{bb}} & -\sqrt{3}\mathrm{R_{bc}} - \mathrm{X_{bc}} \\ -\sqrt{3}\mathrm{R_{ca}} - \mathrm{X_{ca}} & \sqrt{3}\mathrm{R_{cb}} - \mathrm{X_{cb}} & 2\mathrm{X_{cc}} \end{bmatrix} \end{aligned} \quad (6)$$

Generally speaking, the bus voltage magnitude in real DPS under a normal condition is generally around 1.0 p.u. (0.95∼1.05 p.u. in common). Thus, for any $\Delta U = 1 - U(|\Delta U| < 1)$, it has [20],

$$f(\Delta U) = 1/U \approx 1 + \Delta U = 2 - U \quad (7)$$

Introducing (7) into (5), the approximate values of the three-phase voltage drop and the three-phase angle difference can be derived as,

$$\begin{aligned} \mathrm{d}\boldsymbol{U} &= \begin{bmatrix} U_{ia} - U_{oa} \\ U_{ib} - U_{ob} \\ U_{ic} - U_{oc} \end{bmatrix} = \begin{bmatrix} \mathrm{d}U_a \\ \mathrm{d}U_b \\ \mathrm{d}U_c \end{bmatrix} \\ &\approx (\hat{\mathbf{R}}\vec{\boldsymbol{P}}_o + \hat{\mathbf{X}}\vec{\boldsymbol{Q}}_o)) \begin{bmatrix} 2 - U_{oa} \\ 2 - U_{ob} \\ 2 - U_{oc} \end{bmatrix} \end{aligned} \quad (8)$$

$$\mathrm{d}\boldsymbol{\theta} = \begin{bmatrix} \mathrm{d}\theta_a \\ \mathrm{d}\theta_b \\ \mathrm{d}\theta_c \end{bmatrix} \approx \begin{bmatrix} \delta U_a/U_{oa} \\ \delta U_b/U_{ob} \\ \delta U_c/U_{ob} \end{bmatrix} \quad (9)$$

where,

$$\delta\boldsymbol{U} = \begin{bmatrix} \delta U_a \\ \delta U_b \\ \delta U_c \end{bmatrix} \approx (\hat{\mathbf{X}}\vec{\boldsymbol{P}}_o - \hat{\mathbf{R}}\vec{\boldsymbol{Q}}_o) \begin{bmatrix} 2 - U_{oa} \\ 2 - U_{ob} \\ 2 - U_{oc} \end{bmatrix} \quad (10)$$

B. REACTIVE POWER APPROXIMATION OF SHUNT SUSCEPTANCE AND POWER LOSS APPROXIMATION OF BRANCH SERIAL IMPEDANCE

Define $U_\alpha = 1\text{-}\Delta U_\alpha$ and $U_\beta = 1 - \Delta U_\beta$ (α and β refer to phase indexes, a, b, c, at the same or different bus, $\alpha \neq \beta$). As discussed above, the voltage amplitude at each bus for each phase is close to 1 p.u., so $|\Delta U_\alpha|$ and $|\Delta U_\beta|$ are close to zero and $|\Delta U_\alpha \times \Delta U_\beta|$ is much closer to zero. Thus, the following approximate calculation equation can be obtained by neglecting the second-order term, $\Delta U_\alpha \times \Delta U_\beta$.

$$\begin{aligned} U_\alpha U_\beta &= (1-\Delta U_\alpha)(1-\Delta U_\beta) \\ &= 1-\Delta U_\alpha - \Delta U_\beta + \Delta U_\alpha \times \Delta U_\beta \\ &\approx 1-\Delta U_\alpha - \Delta U_\beta = U_\alpha + U_\beta 1 \end{aligned} \tag{11}$$

The shunt susceptance, $\mathbf{B}$ in (2), can be considered as the constant susceptance load. The injected reactive power of $\mathbf{B}$ at any bus can be approximately calculated by,

$$\begin{aligned} \boldsymbol{Q}_{\mathrm{oB}} &= -\mathrm{j}\begin{bmatrix} \dot{U}_{\mathrm{oa}} \\ \dot{U}_{\mathrm{ob}} \\ \dot{U}_{\mathrm{oc}} \end{bmatrix} .* \left\{ \mathbf{B} \begin{bmatrix} \dot{U}^*_{\mathrm{oa}} \\ \dot{U}^*_{\mathrm{ob}} \\ \dot{U}^*_{\mathrm{oc}} \end{bmatrix} \right\} \\ &\approx \frac{-\mathrm{j}}{2} \begin{bmatrix} 2\mathrm{B}_{\mathrm{aa}}U^2_{\mathrm{oa}} - \mathrm{B}_{\mathrm{ab}}U_{\mathrm{oa}}U_{\mathrm{ob}} - \mathrm{B}_{\mathrm{ac}}U_{\mathrm{oa}}U_{\mathrm{oc}} \\ -\mathrm{B}_{\mathrm{ba}}U_{\mathrm{oa}}U_{\mathrm{ob}} + 2\mathrm{B}_{\mathrm{bb}}U^2_{\mathrm{ob}} - \mathrm{B}_{\mathrm{bc}}U_{\mathrm{ob}}U_{\mathrm{oc}} \\ -\mathrm{B}_{\mathrm{ca}}U_{\mathrm{oa}}U_{\mathrm{oc}} - \mathrm{B}_{\mathrm{cb}}U_{\mathrm{ob}}U_{\mathrm{oc}} + 2\mathrm{B}_{\mathrm{cc}}U^2_{\mathrm{oc}} \end{bmatrix} \end{aligned} \tag{12}$$

Based on (11), (12) can be further developed as following,

$$\boldsymbol{Q}_{\mathrm{oB}} \approx -\mathrm{j}[\hat{\mathbf{B}}\boldsymbol{U}_{\mathrm{o}} + \mathrm{diag}(\hat{\mathbf{B}}\boldsymbol{e}_3)\boldsymbol{U}_{\mathrm{o}} - \hat{\boldsymbol{B}}\boldsymbol{e}_3] \tag{13}$$

where, $\hat{\mathbf{B}} = \frac{1}{2}\begin{bmatrix} 2\mathrm{B}_{\mathrm{aa}} & -\mathrm{B}_{\mathrm{ab}} & -\mathrm{B}_{\mathrm{ac}} \\ -\mathrm{B}_{\mathrm{ba}} & 2\mathrm{B}_{\mathrm{bb}} & -\mathrm{B}_{\mathrm{bc}} \\ -\mathrm{B}_{\mathrm{ca}} & -\mathrm{B}_{\mathrm{cb}} & 2\mathrm{B}_{\mathrm{cc}} \end{bmatrix}$ and $\boldsymbol{e}_3 = \begin{bmatrix} 1 \\ 1 \\ 1 \end{bmatrix}$.

Similarly, let $U_{\mathrm{oa}} \approx U_{\mathrm{ob}} \approx U_{\mathrm{ob}} \approx 1$, the power losses of three-phase serial impedance $\mathbf{R} + \mathrm{j}\mathbf{X}$ can be approximately calculated by (here, $\vec{\boldsymbol{P}}_{\mathrm{o}} = \mathrm{diag}(\boldsymbol{P}_{\mathrm{o}})$ and $\vec{\boldsymbol{Q}}_{\mathrm{o}} = \mathrm{diag}(\boldsymbol{Q}_{\mathrm{o}})$),

$$\begin{aligned} \mathrm{d}\boldsymbol{S}_{\mathrm{Z}} &= (\mathrm{d}\boldsymbol{U} + \mathrm{j}\delta\boldsymbol{U}) .* (\boldsymbol{P}_{\mathrm{o}} + \mathrm{j}\boldsymbol{Q}_{\mathrm{o}}) \\ &= [(\hat{\mathbf{R}} + \mathrm{j}\hat{\mathbf{X}})(\vec{\boldsymbol{P}}_{\mathrm{o}} \text{-} \mathrm{j}\vec{\boldsymbol{Q}}_{\mathrm{o}})] .* (\boldsymbol{P}_{\mathrm{o}} + \mathrm{j}\boldsymbol{Q}_{\mathrm{o}}) \\ &\approx (\vec{\boldsymbol{P}}_{\mathrm{o}} + \mathrm{j}\vec{\boldsymbol{Q}}_{\mathrm{o}})(\hat{\mathbf{R}} + \mathrm{j}\hat{\mathbf{X}})(\boldsymbol{P}_{\mathrm{o}} \text{-} \mathrm{j}\boldsymbol{Q}_{\mathrm{o}}) \end{aligned} \tag{14}$$

Expanding (14), the power losses can be approximately formulated as,

$$\begin{cases} \mathrm{d}\boldsymbol{P} = [\mathrm{d}P_{\mathrm{a}}; \mathrm{d}P_{\mathrm{b}}; \mathrm{d}P_{\mathrm{c}}] \\ \qquad \approx \vec{\boldsymbol{P}}_{\mathrm{o}}\hat{\mathbf{R}}\boldsymbol{P}_{\mathrm{o}} + \vec{\boldsymbol{Q}}_{\mathrm{o}}\hat{\mathbf{R}}\boldsymbol{Q}_{\mathrm{o}} + \vec{\boldsymbol{P}}_{\mathrm{o}}\hat{\mathbf{X}}\boldsymbol{Q}_{\mathrm{o}} - \vec{\boldsymbol{Q}}_{\mathrm{o}}\hat{\mathbf{X}}\boldsymbol{P}_{\mathrm{o}} \\ \mathrm{d}Q = [\mathrm{d}Q_{\mathrm{a}}; \mathrm{d}Q_{\mathrm{b}}; \mathrm{d}Q_{\mathrm{c}}] \\ \qquad \approx \vec{\boldsymbol{P}}_{\mathrm{o}}\hat{\mathbf{X}}\boldsymbol{P}_{\mathrm{o}} + \vec{\boldsymbol{Q}}_{\mathrm{o}}\hat{\mathbf{X}}\boldsymbol{Q}_{\mathrm{o}} - \vec{\boldsymbol{P}}_{\mathrm{o}}\hat{\mathbf{R}}\boldsymbol{Q}_{\mathrm{o}} + \vec{\boldsymbol{Q}}_{\mathrm{o}}\hat{\mathbf{R}}\boldsymbol{P}_{\mathrm{o}} \end{cases} \tag{15}$$

C. ZIP LOAD TO IP LOAD APPROXIMATION DEVELOPMENT

For $\mathbf{P}$ type star connection load, it does not need any conversion, so it can define directly,

$$\begin{cases} \boldsymbol{P}_{\mathrm{P}\varphi} = \boldsymbol{P}_{\mathrm{o}} \\ \boldsymbol{Q}_{\mathrm{P}\varphi} = \boldsymbol{Q}_{\mathrm{o}} \end{cases} \tag{16}$$

For the proposed method can only handle the phase-ground loads (star connection load), so for $\mathbf{P}$ type delta connection load, it should be converted to star connection load first. The approximate conversion of delta load, $\boldsymbol{P}_{\mathrm{L}} = [P_{\mathrm{ab}}; P_{\mathrm{bc}}; P_{\mathrm{ca}}]$ and $\boldsymbol{Q}_{\mathrm{L}} = [Q_{\mathrm{ab}}; Q_{\mathrm{bc}}; Q_{\mathrm{ca}}]$, to star load, $\hat{\boldsymbol{P}} = [\hat{P}_{\mathrm{a}}; \hat{P}_{\mathrm{b}}; \hat{P}_{\mathrm{c}}]$ and $\hat{\boldsymbol{Q}} = [\hat{Q}_{\mathrm{a}}; \hat{Q}_{\mathrm{b}}; \hat{Q}_{\mathrm{c}}]$, can be expressed as (the details see equations A.1∼4 in Appendix),

$$\begin{cases} \hat{\boldsymbol{P}} = \dfrac{\mathbf{N}}{2}\boldsymbol{P}_{\mathrm{L}} + \dfrac{\mathbf{M}}{2\sqrt{3}}\boldsymbol{Q}_{\mathrm{L}} \\ \hat{\boldsymbol{Q}} = \dfrac{\mathbf{N}}{2}\boldsymbol{Q}_{\mathrm{L}} - \dfrac{\mathbf{M}}{2\sqrt{3}}\boldsymbol{P}_{\mathrm{L}} \end{cases} \tag{17}$$

where $\mathbf{M} = \begin{bmatrix} 1 & 0 & -1 \\ -1 & 1 & 0 \\ 0 & -1 & 1 \end{bmatrix}$ and $\mathbf{N} = \begin{bmatrix} 1 & 0 & 1 \\ 1 & 1 & 0 \\ 0 & 1 & 1 \end{bmatrix}$.

Then for $\mathbf{P}$ type delta connection load, the conversion can be handled with (17). Then the equivalent phase-ground load can be defined as,

$$\begin{cases} \hat{\boldsymbol{P}}_{\mathrm{P}\varphi} = \hat{\boldsymbol{P}} \\ \hat{\boldsymbol{Q}}_{\mathrm{P}\varphi} = \hat{\boldsymbol{Q}} \end{cases} \tag{18}$$

For $\mathbf{I}$ type star connection load, define $\boldsymbol{P}_{\mathrm{I}} = [P_{\mathrm{Ia}}; P_{\mathrm{Ib}}; P_{\mathrm{Ic}}]$ and $\boldsymbol{Q}_{\mathrm{I}} = [Q_{\mathrm{Ia}}; Q_{\mathrm{Ib}}; Q_{\mathrm{Ic}}]$, $\vec{\boldsymbol{P}}_{\mathrm{I}} = \mathrm{diag}(\boldsymbol{P}_{\mathrm{I}})$ and $\vec{\boldsymbol{Q}}_{\mathrm{I}} = \mathrm{diag}(\boldsymbol{Q}_{\mathrm{I}})$, then it can be written as,

$$\begin{cases} \boldsymbol{P}_{\mathrm{I}} = \boldsymbol{P}_{\mathrm{I}\varphi}\boldsymbol{U}_{\mathrm{o}} = \vec{\boldsymbol{P}}_{\mathrm{I}}\boldsymbol{U}_{\mathrm{o}} \\ \boldsymbol{Q}_{\mathrm{I}} = \boldsymbol{Q}_{\mathrm{I}\varphi}\boldsymbol{U}_{\mathrm{o}} = \vec{\boldsymbol{Q}}_{\mathrm{I}}\boldsymbol{U}_{\mathrm{o}} \end{cases} \tag{19}$$

For $\mathbf{I}$ type delta connection load, $\boldsymbol{P}_{\mathrm{L}}$ and $\boldsymbol{Q}_{\mathrm{L}}$, let $\vec{\boldsymbol{P}}_{\mathrm{L}} = \mathrm{diag}(\boldsymbol{P}_{\mathrm{L}})$ and $\vec{\boldsymbol{Q}}_{\mathrm{L}} = \mathrm{diag}(\boldsymbol{Q}_{\mathrm{L}})$, then the equivalent $\mathbf{I}$ type star connection load $\hat{\boldsymbol{P}}_{\mathrm{I}} = [\hat{P}_{\mathrm{Ia}}; \hat{P}_{\mathrm{Ib}}; \hat{P}_{\mathrm{Ic}}]$ and $\hat{\boldsymbol{Q}}_{\mathrm{I}} = [\hat{Q}_{\mathrm{Ioa}}; \hat{Q}_{\mathrm{Iob}}; \hat{Q}_{\mathrm{Ioc}}]$ can be expressed as (superscript "T" means matrix transpose and the details see equations A.5∼6 in Appendix),

$$\begin{cases} \hat{\boldsymbol{P}}_{\mathrm{I}} = \hat{\boldsymbol{P}}_{\mathrm{I}\varphi}\boldsymbol{U}_{\mathrm{o}} \approx \dfrac{1}{12}\Big(3\mathbf{N}\vec{\boldsymbol{P}}_{\mathrm{L}}\mathbf{N}^{\mathrm{T}} - \sqrt{3}\mathbf{N}\vec{\boldsymbol{Q}}_{\mathrm{L}}\mathbf{M}^{\mathrm{T}} \\ \qquad + \mathbf{M}\vec{\boldsymbol{P}}_{\mathrm{L}}\mathbf{M}^{\mathrm{T}} + \sqrt{3}\mathbf{M}\vec{\boldsymbol{Q}}_{\mathrm{L}}\mathbf{N}^{\mathrm{T}}\Big)\boldsymbol{U}_{\mathrm{o}} \\ \hat{\boldsymbol{Q}}_{\mathrm{I}} = \hat{\boldsymbol{Q}}_{\mathrm{I}\varphi}\boldsymbol{U}_{\mathrm{o}} \approx \dfrac{1}{12}\Big(3\mathbf{N}\vec{\boldsymbol{Q}}_{\mathrm{L}}\mathbf{N}^{\mathrm{T}} + \sqrt{3}\mathbf{N}\vec{\boldsymbol{P}}_{\mathrm{L}}\mathbf{M}^{\mathrm{T}} \\ \qquad + \mathbf{M}\vec{\boldsymbol{Q}}_{\mathrm{L}}\mathbf{M}^{\mathrm{T}} - \sqrt{3}\mathbf{M}\vec{\boldsymbol{P}}_{\mathrm{L}}\mathbf{N}^{\mathrm{T}}\Big)\boldsymbol{U}_{\mathrm{o}} \end{cases} \tag{20}$$

For $\mathbf{Z}$ type star connection load, based on (11), it can derive and define the following equations,

$$\begin{cases} \boldsymbol{P}_{\mathrm{Z}\varphi} = \boldsymbol{P}_{\mathrm{Zi}\varphi}\boldsymbol{U}_{\mathrm{o}} - \boldsymbol{P}_{\mathrm{Zp}\varphi} = \vec{\boldsymbol{P}}_{\mathrm{o}}(\boldsymbol{U}_{\mathrm{o}} .* \boldsymbol{U}_{\mathrm{o}}) \\ \qquad \approx \vec{\boldsymbol{P}}_{\mathrm{o}}(2\boldsymbol{U}_{\mathrm{o}} - e_3) = 2\vec{\boldsymbol{P}}_{\mathrm{o}}\boldsymbol{U}_{\mathrm{o}} - \boldsymbol{P}_{\mathrm{o}} \\ \boldsymbol{Q}_{\mathrm{Z}\varphi} = \boldsymbol{Q}_{\mathrm{Zi}\varphi}\boldsymbol{U}_{\mathrm{o}} - \boldsymbol{Q}_{\mathrm{Zp}\varphi} = \vec{\boldsymbol{Q}}_{\mathrm{o}}(\boldsymbol{U}_{\mathrm{o}} .* \boldsymbol{U}_{\mathrm{o}}) \\ \qquad \approx \vec{\boldsymbol{Q}}_{\mathrm{o}}(2\boldsymbol{U}_{\mathrm{o}} - e_3) = 2\vec{\boldsymbol{Q}}_{\mathrm{o}}\boldsymbol{U}_{\mathrm{o}} - \boldsymbol{Q}_{\mathrm{o}} \end{cases} \tag{21}$$

Aiming at $\mathbf{Z}$ type delta connection load, $\boldsymbol{P}_{\mathrm{L}}$ and $\boldsymbol{Q}_{\mathrm{L}}$ the equivalent $\mathbf{Z}$ type star connection load, $\hat{\boldsymbol{P}}_{\mathrm{Z}} = [\hat{P}_{\mathrm{Za}}; \hat{P}_{\mathrm{Zb}}; \hat{P}_{\mathrm{Zc}}]$ and $\hat{\boldsymbol{Q}}_{\mathrm{Z}\varphi} = [\hat{Q}_{\mathrm{Za}}; \hat{Q}_{\mathrm{Zb}}; \hat{Q}_{\mathrm{Zc}}]$, can be expressed as (the details

see equations A.7∼9 in Appendix),

$$\begin{cases} \hat{\boldsymbol{P}}_{\mathrm{Z}} = \hat{\boldsymbol{P}}_{\mathrm{Zi}\varphi}\boldsymbol{U}_{\mathrm{o}} - \hat{\boldsymbol{P}}_{\mathrm{Zp}\varphi} \approx \dfrac{1}{2}\left[\left(\mathbf{N}\vec{\boldsymbol{P}}_{\mathrm{L}} + \dfrac{1}{\sqrt{3}}\mathbf{M}\vec{\boldsymbol{Q}}_{\mathrm{L}}\right)\mathbf{N}^{\mathrm{T}}\boldsymbol{U}_{\mathrm{o}} - \left(\mathbf{N}\boldsymbol{P}_{\mathrm{L}} + \dfrac{1}{\sqrt{3}}\mathbf{M}\boldsymbol{Q}_{\mathrm{L}}\right)\right] \\ \hat{\boldsymbol{Q}}_{\mathrm{Z}} = \hat{\boldsymbol{Q}}_{\mathrm{Zi}\varphi}\boldsymbol{U}_{\mathrm{o}} - \hat{\boldsymbol{Q}}_{\mathrm{Zp}\varphi} \approx \dfrac{1}{2}\left[\left(\mathbf{N}\mathrm{diag}(\boldsymbol{Q}_{\mathrm{L}}) - \dfrac{1}{\sqrt{3}}\mathbf{M}\vec{\boldsymbol{P}}_{\mathrm{L}}\right) \times\mathbf{N}^{\mathrm{T}}\boldsymbol{U}_{\mathrm{o}} - \left(\mathbf{N}\boldsymbol{Q}_{\mathrm{L}} - \dfrac{1}{\sqrt{3}}\mathbf{M}\boldsymbol{P}_{\mathrm{L}}\right)\right] \end{cases} \tag{22}$$

It can be seen from (21) and (22), based on the approximate calculations, the **Z** type loads are treated as the combination of **I** and **P** type loads.

For any bus j, let $\boldsymbol{P}_{j\Sigma} = [P_{j\sum\mathrm{a}}; P_{j\sum\mathrm{b}}; P_{j\sum\mathrm{c}}]$ and $\boldsymbol{Q}_{j\Sigma} = [Q_{j\sum\mathrm{a}}; Q_{j\sum\mathrm{b}}; Q_{j\sum\mathrm{c}}]$ be the total equivalent IP star connection load, that is, the star and delta connection **ZIP** loads can be combined together with following approximate calculation equations.

$$\begin{cases} \boldsymbol{P}_{j\Sigma} = \vec{\boldsymbol{P}}_{j\mathrm{I}\sum}\boldsymbol{U}_{\mathrm{o}} + \boldsymbol{P}_{j\mathrm{P}\sum} \\ = (\boldsymbol{P}_{\mathrm{I}\varphi} + \hat{\boldsymbol{P}}_{\mathrm{I}\varphi} + \boldsymbol{P}_{\mathrm{Zi}\varphi} + \hat{\boldsymbol{P}}_{\mathrm{Zi}\varphi})\boldsymbol{U}_{\mathrm{o}} \\ \quad + \left(\boldsymbol{P}_{\mathrm{P}\varphi} + \hat{\boldsymbol{P}}_{\mathrm{P}\varphi} - \boldsymbol{P}_{\mathrm{Zp}\varphi} - \hat{\boldsymbol{P}}_{\mathrm{Zi}\varphi}\right) \\ \boldsymbol{Q}_{j\Sigma} = \vec{\boldsymbol{Q}}_{j\mathrm{I}\sum}\boldsymbol{U}_{\mathrm{o}} + \boldsymbol{Q}_{j\mathrm{P}\sum} \\ = (\boldsymbol{Q}_{\mathrm{I}\varphi} + \hat{\boldsymbol{Q}}_{\mathrm{I}\varphi} + \boldsymbol{Q}_{\mathrm{Zi}\varphi} + \hat{\boldsymbol{Q}}_{\mathrm{Zi}\varphi})\boldsymbol{U}_{\mathrm{o}} \\ \quad + \left(\boldsymbol{Q}_{\mathrm{P}\varphi} + \hat{\boldsymbol{Q}}_{\mathrm{P}\varphi} - \boldsymbol{Q}_{\mathrm{Zp}\varphi} - \hat{\boldsymbol{Q}}_{\mathrm{Zi}\varphi}\right) \end{cases} \tag{23}$$

It can be seen from (23) that the hybrid connection ZIP loads are approximated as the star connection IP loads.

III. THE THREE-PHASE UNBALANCED LINEAR SOLUTION

In this section, based on our past works, that is, the single-phase improved loop-analysis theory based power flow methods in [20]–[22], the three-phase unbalanced power flow method is introduced. Then based on the approximate calculations discussed in section II, the proposed LPF method has been developed and proposed.

A. THE PROPOSED POWER FLOW METHOD

For a three-phase weakly-meshed distribution network with 3(N+1) buses and 3m link branches (section lines, to form 3m independent loops), the total branches are 3(N+m). Define $\boldsymbol{Q}_{\mathrm{I}} = [\boldsymbol{Q}_{\mathrm{It}}; \boldsymbol{Q}_{Il}] = [\boldsymbol{Q}_{\mathrm{i}1}; \boldsymbol{Q}_{\mathrm{i}2}; \cdots; \boldsymbol{Q}_{\mathrm{i(N+m)}}]$ ($\boldsymbol{Q}_{ik} = [Q_{ik\mathrm{a}}; Q_{ik\mathrm{b}}; Q_{ik\mathrm{c}}]$) and $\boldsymbol{P}_{\mathrm{I}} = [\boldsymbol{P}_{\mathrm{It}}; \boldsymbol{P}_{Il}] = [\boldsymbol{P}_{\mathrm{i}1}; \boldsymbol{P}_{\mathrm{i}2}; \cdots; \boldsymbol{P}_{\mathrm{i(N+m)}}]$ ($\boldsymbol{P}_{\mathrm{i}k} = [P_{ik\mathrm{a}}; P_{ik\mathrm{b}}; P_{ik\mathrm{c}}]$) be the branch reactive and active power vectors, $\boldsymbol{P} = [\boldsymbol{P}_1; \boldsymbol{P}_2; \cdots; \boldsymbol{P}_{\mathrm{N}}]$ ($\boldsymbol{P}_k = [P_{k\mathrm{a}}; P_{k\mathrm{b}}; P_{k\mathrm{c}}]$) and $\boldsymbol{Q} = [\boldsymbol{Q}_1; \boldsymbol{Q}_2; \cdots; \boldsymbol{Q}_{\mathrm{N}}]$ ($\boldsymbol{Q}_k = [Q_{k\mathrm{a}}; Q_{k\mathrm{b}}; Q_{k\mathrm{c}}]$) be the bus consumption active and reactive power vectors. The bus consumption powers include the loads (herein only consider the $\boldsymbol{P}$ type loads first), the reactive powers of shunt susceptance and the serial branch power loss in the π-models [21], [22]. Then the following equations can be derived for three-phase distribution system similarly as in [21],

$$\begin{cases} \boldsymbol{P}_{\mathrm{It}} = \mathbf{T}_{\mathrm{t}}^{\mathrm{T}}\boldsymbol{P} + \mathbf{B}_{\mathrm{t}}^{\mathrm{T}}\boldsymbol{P}_{Il} \\ \boldsymbol{Q}_{\mathrm{It}} = \mathbf{T}_{\mathrm{t}}^{\mathrm{T}}\boldsymbol{Q} + \mathbf{B}_{\mathrm{t}}^{\mathrm{T}}\boldsymbol{Q}_{Il} \end{cases} \tag{24}$$

where, Tt is path matrix of 3N*3N and Bt is loop matrix of 3m*3N corresponding to the tree branches. The details about $\mathrm{T_t}$ and $\mathrm{B_t}$ for three-phase DPS can be found in [23].

Define $\mathrm{d}\boldsymbol{U}_{\mathrm{t}} = [\mathrm{d}\boldsymbol{U}_1; \mathrm{d}\boldsymbol{U}_2; \cdots; \mathrm{d}\boldsymbol{U}_{\mathrm{N}}]$ ($\mathrm{d}\boldsymbol{U}_k = [\mathrm{d}U_{k\mathrm{a}}; \mathrm{d}U_{k\mathrm{b}}; \mathrm{d}U_{k\mathrm{c}}]$), $\mathbf{U}_{\mathrm{ini}} = [\mathbf{U}_0; \mathbf{U}_0; \cdots; \mathbf{U}_0]$ (3N*1, $\mathbf{U}_0 = [\mathrm{U}_{0\mathrm{a}}; \mathrm{U}_{0\mathrm{b}}; \mathrm{U}_{0\mathrm{c}}]$ is the three-phase source voltage magnitude vector). And then let $\boldsymbol{U}_{\mathrm{n}} = [\boldsymbol{U}_1; \boldsymbol{U}_2; \cdots; \boldsymbol{U}_{\mathrm{N}}]$ ($\boldsymbol{U}_k = [U_{k\mathrm{a}}; U_{k\mathrm{b}}; U_{k\mathrm{c}}]$) be the voltage vector (3N*1). So the voltage magnitude differences between power supply and any other bus at bus k equal to the summation of the tree branch voltage drop along the path of bus k along the same phase, that is [21], [22],

$$\boldsymbol{U}_{\mathrm{n}} = \mathbf{U}_{\mathrm{ini}} - \mathbf{T}_{\mathrm{t}}\mathrm{d}\boldsymbol{U}_{\mathrm{t}} \tag{25}$$

Define the angles of power supply (source bus), $\boldsymbol{\theta}_{\mathrm{ini}} = [\boldsymbol{\theta}_0; \boldsymbol{\theta}_0; \cdots; \boldsymbol{\theta}_0]$ (3N*1, $\boldsymbol{\theta}_0 = [\theta_{0\mathrm{a}}; \theta_{0\mathrm{b}}; \theta_{0\mathrm{c}}]$ is the three-phase reference angle vector). And let $\boldsymbol{\theta}_{\mathrm{n}} = [\boldsymbol{\theta}_1; \boldsymbol{\theta}_2; \cdots; \boldsymbol{\theta}_{\mathrm{N}}]$ ($\boldsymbol{\theta}_k = [\boldsymbol{\theta}_{k\mathrm{a}}; \boldsymbol{\theta}_{k\mathrm{b}}; \boldsymbol{\theta}_{k\mathrm{c}}]$) be the bus voltage angle vector (3N*1). Define $\mathrm{d}\boldsymbol{\theta}_{\mathrm{t}} = [\mathrm{d}\boldsymbol{\theta}_1; \mathrm{d}\boldsymbol{\theta}_2; \cdots; \mathrm{d}\boldsymbol{\theta}_{\mathrm{N}}]$ ($\mathrm{d}\boldsymbol{\theta}_k = [\mathrm{d}\theta_{k\mathrm{a}}; \mathrm{d}\theta_{k\mathrm{b}}; \mathrm{d}\theta_{k\mathrm{c}}]$). Then, similarly, there is [21], [22],

$$\boldsymbol{\theta}_{\mathrm{n}} = \boldsymbol{\theta}_{\mathrm{ini}} - \mathbf{T}_{\mathrm{t}}\mathrm{d}\boldsymbol{\theta}_{\mathrm{t}} \tag{26}$$

Based on (8), in matrix and vector form, it has,

$$\mathrm{d}\boldsymbol{U}_{\mathrm{t}} \approx \mathrm{diag}(\hat{\mathbf{R}}_{\mathrm{t}}\boldsymbol{P}_{\mathrm{It}} + \hat{\mathbf{X}}_{\mathrm{t}}\boldsymbol{Q}_{\mathrm{It}})(2 - \boldsymbol{U}_{\mathrm{n}}) \tag{27}$$

And then the linear power flow calculation formula can be obtained by introducing (27) into (25). Now, it needs to get $\boldsymbol{P}_{\mathrm{It}}$ and $\boldsymbol{Q}_{\mathrm{It}}$ with (24), but the key is to calculate $\boldsymbol{P}_{Il}$ and $\boldsymbol{Q}_{Il}$ in (24)

The branch power losses in the bus consumption active and reactive powers can be approximately calculated by doing a backward sweep calculation with only considering the radial network by breaking up the links. That is, $\boldsymbol{P}_{\mathrm{Il}} = \mathbf{T}_{\mathrm{t}}^{\mathrm{T}}\boldsymbol{P}$ and $\boldsymbol{Q}_{\mathrm{Il}} = \mathbf{T}_{\mathrm{t}}^{\mathrm{T}}\boldsymbol{Q}$. Here the contributions of the bus injection powers $\boldsymbol{P}$ and $\boldsymbol{Q}$ (all loads are treated as $\boldsymbol{P}$ type load and no branch power losses are included) are only considered. Then the branch power losses can be approximately calculated with (15) by setting all bus voltage magnitudes be 1.0 p.u..

B. THE APPROXIMATION CALCULATION OF LINK POWERS

Let $\hat{\mathbf{R}}_{\mathrm{t}}$ (3N*3N) and $\hat{\mathbf{R}}_l$ (3M*3M) be the tree-branch and loop-link resistance diagonal matrix respectively, $\hat{\mathbf{X}}_{\mathrm{t}}$ (3N*3N) and $\hat{\mathbf{X}}_l$ (3M*3M) be the tree-branch and link reactance diagonal matrix respectively (the diagonal elements are the equivalent branch parameter matrix, $\hat{\mathbf{R}}$ and $\hat{\mathbf{X}}$are calculated based on (6)).

It considers that the contribution ratio of link powers to $\boldsymbol{P}_{\mathrm{It}}$ and $\boldsymbol{Q}_{\mathrm{It}}$ is relatively small because of the weakly meshed characteristic of the distribution network, so all loads, either **I** type load or **Z** type load, are treated as the $\boldsymbol{P}$ type load for the approximation calculation of link powers. But for the delta

connection load, the equivalent star connection results should be calculated with (17) first.

1) THE HANDLING OF LOOP LINKS

Let $\mathrm{d}\boldsymbol{U}_l = [\mathrm{d}\boldsymbol{U}_{l1}; \mathrm{d}\boldsymbol{U}_{l2}; \cdots; \mathrm{d}\boldsymbol{U}_{l\mathrm{m}}]$ ($\mathrm{d}\boldsymbol{U}_{lj} = [\mathrm{d}U_{lj\mathrm{a}}; \mathrm{d}U_{lj\mathrm{b}}; \mathrm{d}U_{lj\mathrm{c}}]$) be link voltage drop vector and $\mathrm{d}\boldsymbol{\theta}_l = [\mathrm{d}\boldsymbol{\theta}_{l1}; \mathrm{d}\boldsymbol{\theta}_{l2}; \cdots; \mathrm{d}\boldsymbol{\theta}_{l\mathrm{m}}]$ ($\mathrm{d}\boldsymbol{\theta}_{lj} = [\mathrm{d}\theta_{lj\mathrm{a}}; \mathrm{d}\theta_{lj\mathrm{b}}; \mathrm{d}\theta_{lj\mathrm{c}}]$) be angle difference vector for the loop branches. Based on Kirchhoff's voltage law, there are,

$$\mathbf{B}_\mathrm{t}\mathrm{d}\boldsymbol{U}_\mathrm{t} + \mathrm{d}\boldsymbol{U}_l = 0 \tag{28}$$

$$\mathbf{B}_\mathrm{t}\mathrm{d}\boldsymbol{\theta}_\mathrm{t} + \mathrm{d}\boldsymbol{\theta}_l = 0 \tag{29}$$

Considering that the voltage magnitude at each bus is close to the rated value, 1.0 p.u.. Thus, the following approximations can be derived based on (8) & (9) by supposing all voltage magnitudes be 1.0 p.u.. When the voltages are not bad, it still has a relatively higher accuracy.

$$\mathrm{d}\boldsymbol{U} \approx (\hat{\mathbf{R}}\boldsymbol{P}_\mathrm{o} + \hat{\mathbf{X}}\boldsymbol{Q}_\mathrm{o}) \tag{30}$$

$$\mathrm{d}\boldsymbol{\theta} \approx (\hat{\mathbf{X}}\boldsymbol{P}_\mathrm{o} - \hat{\mathbf{R}}\boldsymbol{Q}_\mathrm{o}) \tag{31}$$

Then based on (28) and (29) the following equations can be obtained [22],

$$\begin{cases} \mathbf{B}_\mathrm{t}\mathrm{d}\boldsymbol{U}_\mathrm{t} = \mathbf{B}_\mathrm{t}[\hat{\mathbf{R}}_\mathrm{t}(\mathbf{T}_\mathrm{t}^\mathrm{T}\boldsymbol{P} + \mathbf{B}_\mathrm{t}^\mathrm{T}\boldsymbol{P}_{Il}) + \hat{\mathbf{X}}_\mathrm{t}(\mathbf{T}_\mathrm{t}^\mathrm{T}\boldsymbol{Q} + \mathbf{B}_\mathrm{t}^\mathrm{T}\boldsymbol{Q}_{Il})] \\ = -\mathrm{d}\boldsymbol{U}_l = -(\hat{\mathbf{R}}_l\boldsymbol{P}_{Il} + \hat{\mathbf{X}}_l\boldsymbol{Q}_{Il}) \\ \mathbf{B}_\mathrm{t}\mathrm{d}\boldsymbol{\theta}_\mathrm{t} = \mathbf{B}_\mathrm{t}[\hat{\mathbf{X}}_\mathrm{t}(\mathbf{T}_\mathrm{t}^\mathrm{T}\boldsymbol{P} + \mathbf{B}_\mathrm{t}^\mathrm{T}\boldsymbol{P}_{Il}) - \hat{\mathbf{R}}_\mathrm{t}(\mathbf{T}_\mathrm{t}^\mathrm{T}\boldsymbol{Q} + \mathbf{B}_\mathrm{t}^\mathrm{T}\boldsymbol{Q}_{Il})] \\ = -\mathrm{d}\boldsymbol{\theta}_l = -(\hat{\mathbf{X}}_l\boldsymbol{P}_{Il} - \hat{\mathbf{R}}_l\boldsymbol{Q}_{Il}) \end{cases} \tag{32}$$

Rearranging (32) in matrix form,

$$\begin{bmatrix} \hat{\mathbf{R}}_\mathrm{L} & \hat{\mathbf{X}}_\mathrm{L} \\ \hat{\mathbf{X}}_\mathrm{L} & -\hat{\mathbf{R}}_\mathrm{L} \end{bmatrix} \begin{bmatrix} \boldsymbol{P}_{Il} \\ \boldsymbol{Q}_{Il} \end{bmatrix} = \begin{bmatrix} -\hat{\mathbf{R}}_\mathrm{BT} & -\hat{\mathbf{X}}_\mathrm{BT} \\ -\hat{\mathbf{X}}_\mathrm{BT} & \hat{\mathbf{R}}_\mathrm{BT} \end{bmatrix} \begin{bmatrix} \boldsymbol{P} \\ \boldsymbol{Q} \end{bmatrix} \tag{33}$$

where, $\hat{\mathbf{R}}_\mathrm{BT} = \mathbf{B}_\mathrm{t}\hat{\mathbf{R}}_\mathrm{t}\mathbf{T}_\mathrm{t}^\mathrm{T}$, $\hat{\mathbf{X}}_\mathrm{BT} = \mathbf{B}_\mathrm{t}\hat{\mathbf{X}}_\mathrm{t}\mathbf{T}_\mathrm{t}^\mathrm{T}$, $\hat{\mathbf{R}}_\mathrm{L} = \hat{\mathbf{R}}_l + \mathbf{B}_\mathrm{t}\hat{\mathbf{R}}_\mathrm{t}\mathbf{B}_\mathrm{t}^\mathrm{T}$, $\hat{\mathbf{X}}_\mathrm{L} = \hat{\mathbf{X}}_l + \mathbf{B}_\mathrm{t}\hat{\mathbf{X}}_\mathrm{t}\mathbf{B}_\mathrm{t}^\mathrm{T}$.

2) THE HANDLING OF PV BUSES

The distributed generators (DGs) with unity or fixed power factor can be treated as the negative loads in the proposed method. But the PV buses can't be dealt with directly. However, the missing voltage angle set point also makes it possible to transform a PV generator into an artificial loop by one artificial lossless line [22]. Define ($\mathrm{N_{PV}}$ is the number of PV type DG),

$$\mathrm{d}U_{\mathrm{PV}\varphi} = U_{\mathrm{PV}\varphi} - U_{0\varphi}(k = 1, 2, \cdots, \mathrm{N_{PV}}; \varphi = \mathrm{a,b,c}) \tag{34}$$

Extracting all PV buses corresponding row vectors from path matrices $\mathbf{T}_\mathrm{t}$ makes up a new matrix $\mathbf{T}_\mathrm{PV}$ ($3\mathrm{N_{PV}}*3\mathrm{N}$). Considering that the active powers from PV bus are known and invariable, that is, $\boldsymbol{P}_\mathrm{IPV} = \mathbf{const}$. Similarly, for approximate calculation, let $U_{\mathrm{i}\varphi} \approx U_{\mathrm{o}\varphi} \approx 1$, then,

$$\begin{aligned} \mathrm{d}\boldsymbol{U}_\mathrm{PV} &= -\mathbf{T}_\mathrm{PV}\mathrm{d}\boldsymbol{U}_\mathrm{t} \\ &= -\mathbf{T}_\mathrm{PV}[\hat{\mathbf{R}}_\mathrm{t}(\mathbf{T}_\mathrm{t}^\mathrm{T}\boldsymbol{P} + \mathbf{T}_\mathrm{PV}^\mathrm{T}\boldsymbol{P}_\mathrm{IPV}) \\ &\quad + \hat{\mathbf{X}}_\mathrm{t}(\mathbf{T}_\mathrm{t}^\mathrm{T}\boldsymbol{Q} + \mathbf{T}_\mathrm{PV}^\mathrm{T}\boldsymbol{Q}_\mathrm{IPV})] \end{aligned} \tag{35}$$

Rearranging (35), it gives,

$$\hat{\mathbf{X}}_\mathrm{PV}\boldsymbol{Q}_\mathrm{IPV} = \begin{bmatrix} -\hat{\mathbf{R}}_\mathrm{PT} & -\hat{\mathbf{X}}_\mathrm{PT} \end{bmatrix} \begin{bmatrix} \boldsymbol{P} \\ \boldsymbol{Q} \end{bmatrix} - \hat{\mathbf{R}}_\mathrm{PV}\boldsymbol{P}_\mathrm{IPV} - \mathrm{d}\boldsymbol{U}_\mathrm{PV} \tag{36}$$

where, $\hat{\mathbf{X}}_\mathrm{PT} = \mathbf{T}_\mathrm{PV}\hat{\mathbf{X}}_\mathrm{t}\mathbf{T}_\mathrm{t}^\mathrm{T}$, $\hat{\mathbf{R}}_\mathrm{PT} = \mathbf{T}_\mathrm{PV}\hat{\mathbf{R}}_\mathrm{t}\mathbf{T}_\mathrm{t}^\mathrm{T}$, $\hat{\mathbf{X}}_\mathrm{PV} = \mathbf{T}_\mathrm{PV}\hat{\mathbf{X}}_\mathrm{t}\mathbf{T}_\mathrm{PV}^\mathrm{T}$, $\hat{\mathbf{R}}_\mathrm{PV} = \mathbf{T}_\mathrm{PV}\hat{\mathbf{R}}_\mathrm{t}\mathbf{T}_\mathrm{PV}^\mathrm{T}$.

It needs to note that the output reactive power is limited for each PV bus. If the calculated reactive power violates the upper or lower limit, it will be directly set to upper or lower limit. And then the PV bus will be treated as a negative PQ bus.

3) COMBINATION

Let $\hat{\mathbf{X}}_\mathrm{BP} = \mathbf{B}_\mathrm{t}\hat{\mathbf{X}}_\mathrm{t}\mathbf{T}_\mathrm{PV}^\mathrm{T}$ and $\hat{\mathbf{R}}_\mathrm{BP} = \mathbf{B}_\mathrm{t}\hat{\mathbf{R}}_\mathrm{t}\mathbf{T}_\mathrm{PV}^\mathrm{T}$, the loops and PV buses can be combined together as,

$$\begin{bmatrix} \hat{\mathbf{R}}_\mathrm{L} & \hat{\mathbf{X}}_\mathrm{L} & \hat{\mathbf{X}}_\mathrm{BP} \\ \hat{\mathbf{R}}_\mathrm{BP}^\mathrm{T} & \hat{\mathbf{X}}_\mathrm{BP}^\mathrm{T} & \hat{\mathbf{X}}_\mathrm{PV} \\ \hat{\mathbf{X}}_\mathrm{L} & -\hat{\mathbf{R}}_\mathrm{L} & -\hat{\mathbf{R}}_\mathrm{BP} \end{bmatrix} \begin{bmatrix} \boldsymbol{P}_{Il} \\ \boldsymbol{Q}_{Il} \\ \boldsymbol{Q}_\mathrm{IPV} \end{bmatrix} = -\begin{bmatrix} \hat{\mathbf{R}}_\mathrm{BT} & \hat{\mathbf{X}}_\mathrm{BT} \\ \hat{\mathbf{R}}_\mathrm{PT} & \hat{\mathbf{X}}_\mathrm{PT} \\ \hat{\mathbf{X}}_\mathrm{BT} & -\hat{\mathbf{R}}_\mathrm{BT} \end{bmatrix} \begin{bmatrix} \boldsymbol{P} \\ \boldsymbol{Q} \end{bmatrix} - \begin{bmatrix} \hat{\mathbf{R}}_\mathrm{BP} \\ \hat{\mathbf{R}}_\mathrm{PV} \\ \hat{\mathbf{X}}_\mathrm{BP} \end{bmatrix} \boldsymbol{P}_\mathrm{IPV} - \begin{bmatrix} \mathbf{0}_\mathrm{BP} \\ \mathrm{d}\mathbf{U}_{PV} \\ \mathbf{0}_\mathrm{BP} \end{bmatrix} \tag{37}$$

Based on (37), it can derive,

$$\begin{bmatrix} \boldsymbol{P}_{Il} \\ \boldsymbol{Q}_{Il} \\ \boldsymbol{Q}_\mathrm{IPV} \end{bmatrix} = -\begin{bmatrix} \hat{\mathbf{R}}_\mathrm{L} & \hat{\mathbf{X}}_\mathrm{L} & \hat{\mathbf{X}}_\mathrm{BP} \\ \hat{\mathbf{R}}_\mathrm{BP}^\mathrm{T} & \hat{\mathbf{X}}_\mathrm{BP}^\mathrm{T} & \hat{\mathbf{X}}_\mathrm{PV} \\ \hat{\mathbf{X}}_\mathrm{L} & -\hat{\mathbf{R}}_\mathrm{L} & -\hat{\mathbf{R}}_\mathrm{BP} \end{bmatrix}^{-1} \left\{ \begin{bmatrix} \hat{\mathbf{R}}_\mathrm{BT} & \hat{\mathbf{X}}_\mathrm{BT} \\ \hat{\mathbf{R}}_\mathrm{PT} & \hat{\mathbf{X}}_\mathrm{PT} \\ \hat{\mathbf{X}}_\mathrm{BT} & -\hat{\mathbf{R}}_\mathrm{BT} \end{bmatrix} \begin{bmatrix} \boldsymbol{P} \\ \boldsymbol{Q} \end{bmatrix} - \begin{bmatrix} \hat{\mathbf{R}}_\mathrm{BP} \\ \hat{\mathbf{R}}_\mathrm{PV} \\ \hat{\mathbf{X}}_\mathrm{BP} \end{bmatrix} \boldsymbol{P}_\mathrm{IPV} - \begin{bmatrix} \mathbf{0} \\ \mathrm{d}\mathbf{U}_{PV} \\ \mathbf{0} \end{bmatrix} \right\} \tag{38}$$

C. THE REALIZATION OF THE PROPOSED LPF (LALPF)

Including the PV buses into (24), then rewriting (24),

$$\begin{cases} \boldsymbol{P}_\mathrm{It} = \mathbf{T}_\mathrm{t}^\mathrm{T}\boldsymbol{P} + \mathbf{B}_\mathrm{t}^\mathrm{T}\boldsymbol{P}_{Il} + \mathbf{T}_\mathrm{PV}^\mathrm{T}\boldsymbol{P}_\mathrm{IPV} \\ \boldsymbol{Q}_\mathrm{It} = \mathbf{T}_\mathrm{t}^\mathrm{T}\boldsymbol{Q} + \mathbf{B}_\mathrm{t}^\mathrm{T}\boldsymbol{Q}_{Il} + \mathbf{T}_\mathrm{PV}^\mathrm{T}\boldsymbol{Q}_\mathrm{IPV} \end{cases} \tag{39}$$

$\boldsymbol{P}_{Il}$ and $\boldsymbol{Q}_{Il}, \boldsymbol{Q}_\mathrm{IPV}$ can be solved with (38) and then substituting the results into (39), $\boldsymbol{P}_\mathrm{It}$ and $\boldsymbol{Q}_\mathrm{It}$ are obtained. Thus, when just considering **P** type loads, based on (25) and (27), it has,

$$\boldsymbol{U}_\mathrm{n} = \mathbf{U}_\mathrm{ini} - \mathbf{T}_\mathrm{t}\mathrm{d}\boldsymbol{U}_\mathrm{t} \approx \mathbf{U}_\mathrm{ini} - \mathbf{T}_\mathrm{t}\mathrm{diag}(\hat{\mathbf{R}}_\mathrm{t}\vec{\boldsymbol{P}}_\mathrm{It} + \hat{\mathbf{X}}_\mathrm{t}\vec{\boldsymbol{Q}}_\mathrm{It})(2 - \boldsymbol{U}_\mathrm{n}) \tag{40}$$

Rearrange (40) and write it with a simple matrix form,

$$\boldsymbol{H}\boldsymbol{U}_\mathrm{n} = b \tag{41}$$

where,

$$\boldsymbol{H} = \mathbf{E} - \mathbf{T}_\mathrm{t}\mathrm{diag}(\hat{\mathbf{R}}_\mathrm{t}\vec{\boldsymbol{P}}_\mathrm{It} + \hat{\mathbf{X}}_\mathrm{t}\vec{\boldsymbol{Q}}_\mathrm{It}) \tag{42}$$

$$\boldsymbol{b} = \mathbf{U}_\mathrm{ini} - 2\mathbf{T}_\mathrm{t}(\hat{\mathbf{R}}_\mathrm{t}\boldsymbol{P}_\mathrm{It} + \hat{\mathbf{X}}_\mathrm{t}\boldsymbol{Q}_\mathrm{It}) \tag{43}$$

Based on (41), the linear power solution for voltage magnitudes can be solved directly. And the angles can be calculated with (9), (10) and (29).

In (41), $\mathbf{T}_t$ is a lower triangular matrix. By taking a 3*3 matrix (like $\hat{\mathbf{R}}$ and $\hat{\mathbf{X}}$ in (6)) as a basic element in the coefficient matrix, it can be easy to prove that $\boldsymbol{H}$ is a lower triangular matrix too. Thus, $\boldsymbol{U}_n$ can be easily solved with elimination method based on a simple iterative process. Moreover, compared with most LPFs in [11]–[13], [18], [19] under rectangular coordinates and polar coordinates, their coefficient matrixes are 6N*6N matrixes, but the proposed model has a 3N*3N coefficient matrix $\boldsymbol{H}$.

Referring to (27), define $\boldsymbol{P}_{P\Sigma} = [\boldsymbol{P}_{1P\Sigma}; \boldsymbol{P}_{2P\sum}; \cdots; \boldsymbol{P}_{NP\sum}]$ ($\boldsymbol{P}_{jP\Sigma} = [P_{jP\sum a}; P_{jP\sum b}; P_{jP\sum c}]$) and $\boldsymbol{Q}_{P\Sigma} = [\boldsymbol{Q}_{1P\Sigma}; \boldsymbol{Q}_{2P\sum}; \cdots; \boldsymbol{Q}_{NP\sum}]$ ($\boldsymbol{Q}_{jP\Sigma} = [Q_{jP\sum a}; Q_{jP\sum b}; Q_{jP\sum c}]$), $\vec{\boldsymbol{P}}_{I\sum} = \text{diag}([P_{1I\Sigma}; P_{2I\Sigma}; \ldots; P_{NI\Sigma}])$ ($\boldsymbol{P}_{jI\Sigma} = [P_{jI\Sigma a}; P_{jI\Sigma b}; P_{jI\Sigma c}]$) and $\vec{\boldsymbol{Q}}_{I\sum} = \text{diag}([\boldsymbol{Q}_{1I\Sigma}; \boldsymbol{Q}_{2I\Sigma}; \ldots; \boldsymbol{Q}_{NI\Sigma}])$ ($\boldsymbol{Q}_{jI\Sigma} = [Q_{jI\Sigma a}; Q_{jI\Sigma b}; Q_{jI\Sigma c}]$). Then when considering **ZIP** type loads, (39) can be rewritten as,

$$\begin{cases} \boldsymbol{P}_{It} = \mathbf{T}_t^T(\vec{\boldsymbol{P}}_{I\sum}\boldsymbol{U}_n + \boldsymbol{P}_{P\sum}) + \mathbf{B}_t^T\boldsymbol{P}_{Il} + \mathbf{T}_{PV}^T\boldsymbol{P}_{IPV} \\ = \mathbf{T}_t^T\vec{\boldsymbol{P}}_{I\sum}\boldsymbol{U}_n + (\mathbf{T}_t^T\boldsymbol{P}_{P\sum} + \mathbf{B}_t^T\boldsymbol{P}_{Il} + \mathbf{T}_{PV}^T\boldsymbol{P}_{IPV}) \\ \boldsymbol{Q}_{It} = \mathbf{T}_t^T(\vec{\boldsymbol{Q}}_{I\sum}\boldsymbol{U}_n + \boldsymbol{Q}_{P\sum}) + \mathbf{B}_t^T\boldsymbol{Q}_{Il} + \mathbf{T}_{PV}^T\boldsymbol{Q}_{IPV} \\ = \mathbf{T}_t^T\vec{\boldsymbol{Q}}_{I\sum}\boldsymbol{U}_n + (\mathbf{T}_t^T\boldsymbol{Q}_{P\sum} + \mathbf{B}_t^T\boldsymbol{Q}_{Il} + \mathbf{T}_{PV}^T\boldsymbol{Q}_{IPV}) \end{cases} \tag{44}$$

Based on (44), it has

$$\begin{aligned} &\hat{\mathbf{R}}_t\boldsymbol{P}_{It} + \hat{\mathbf{X}}_t\boldsymbol{Q}_{It} \\ &= \hat{R}t[\mathbf{T}_t^T\vec{P}_{I\sum}\boldsymbol{U}_n + (\mathbf{T}_t^T\boldsymbol{P}_{P\sum} + \mathbf{B}_t^T\boldsymbol{P}_{Il} + \mathbf{T}_{PV}^T\boldsymbol{P}_{IPV})] \\ &\quad + \hat{\mathbf{X}}_t[\mathbf{T}_t^T\vec{\boldsymbol{Q}}_{I\sum}\boldsymbol{U}_n + (\mathbf{T}_t^T\boldsymbol{Q}_{P\sum} + \mathbf{B}_t^T\boldsymbol{Q}_{Il} + \mathbf{T}_{PV}^T\boldsymbol{Q}_{IPV})] \end{aligned} \tag{45}$$

Rearrange (45) and write it with a simple matrix form

$$\hat{\mathbf{R}}_t\boldsymbol{P}_{It} + \hat{\mathbf{X}}_t\boldsymbol{Q}_{It} = \boldsymbol{\Gamma}_I\boldsymbol{U}_n + \boldsymbol{\Gamma}_p \tag{46}$$

where,

$$\boldsymbol{\Gamma}_I = \hat{\mathbf{R}}_t\mathbf{T}_t^T\vec{\boldsymbol{P}}_{I\sum} + \hat{\mathbf{X}}_t\mathbf{T}_t^T\vec{\boldsymbol{Q}}_{I\sum} \tag{47}$$

$$\begin{aligned} \boldsymbol{\Gamma}_p &= \hat{\mathbf{R}}_t(\mathbf{T}_t^T\boldsymbol{P}_{P\sum} + \mathbf{B}_t^T\boldsymbol{P}_{Il} + \mathbf{T}_{PV}^T\boldsymbol{P}_{IPV}) \\ &\quad + \hat{\mathbf{X}}_t(\mathbf{T}_t^T\boldsymbol{Q}_{P\sum} + \mathbf{B}_t^T\boldsymbol{Q}_{Il} + \mathbf{T}_{PV}^T\boldsymbol{Q}_{IPV}) \end{aligned} \tag{48}$$

Then based on (27), it can derive,

$$\begin{aligned} \text{d}\boldsymbol{U}_t &\approx \text{diag}(\hat{\mathbf{R}}_t\vec{\boldsymbol{P}}_{It} + \hat{\mathbf{X}}_t\vec{\boldsymbol{Q}}_{It})(2\boldsymbol{e}_N - \boldsymbol{U}_n) \\ &= \text{-diag}(\boldsymbol{\Gamma}_I\boldsymbol{U}_n)\boldsymbol{U}_n + [2\boldsymbol{\Gamma}_I\text{-diag}(\boldsymbol{\Gamma}_p)]\boldsymbol{U}_n + 2\boldsymbol{\Gamma}_p \end{aligned} \tag{49}$$

Based on (11), $U_\alpha U_\beta \approx U_\alpha + U_\beta - 1$, it can derive,

$$\text{diag}(\boldsymbol{\Gamma}_I\boldsymbol{U}_n)\boldsymbol{U}_n \approx \text{diag}(\boldsymbol{\Gamma}_I\boldsymbol{e}_N)\boldsymbol{U}_n + \boldsymbol{\Gamma}_I\boldsymbol{U}_n - \boldsymbol{\Gamma}_I\boldsymbol{e}_N \tag{50}$$

where,$\boldsymbol{e}_N$ is a 3N*1 column vector with all ones.

Substituting (50) into (49) and rearranging it, then,

$$\text{d}\boldsymbol{U}_t = \boldsymbol{\Xi}_I\boldsymbol{U}_n + \boldsymbol{\Xi}_p \approx [\boldsymbol{\Gamma}_I\text{-diag}(\boldsymbol{\Gamma}_p + \boldsymbol{\Gamma}_I\boldsymbol{e}_N)]\boldsymbol{U}_n + 2\boldsymbol{\Gamma}_p + \boldsymbol{\Gamma}_I\boldsymbol{e}_N \tag{51}$$

where,

$$\boldsymbol{\Xi}_I = \boldsymbol{\Gamma}_I\text{-diag}(\boldsymbol{\Gamma}_p + \boldsymbol{\Gamma}_I\boldsymbol{e}_N) \tag{52}$$

$$\boldsymbol{\Xi}_p = 2\boldsymbol{\Gamma}_p + \boldsymbol{\Gamma}_I\boldsymbol{e}_N \tag{53}$$

And substituting (51) into (25), then the linear power equations with ZIP loads can be expressed as follows,

$$(\mathbf{E}_N + \mathbf{T}_t\boldsymbol{\Xi}_I)\boldsymbol{U}_n = \mathbf{U}_{ini} - \mathbf{T}_t\boldsymbol{\Xi}_p \tag{54}$$

The angles can be also calculated with (9), (10) and (29). The same as (41), the coefficient matrix ($\mathbf{E}_N + \mathbf{T}_t\boldsymbol{\Xi}_I$) in (54) is also a 3N*3N matrix. But different from (41), the coefficient matrix ($\mathbf{E}_N + \mathbf{T}_t\boldsymbol{\Xi}_I$) is a sparse matrix but not a triangular matrix, so it will spend a little more time to solve (54) than to solve (41).

The flow chart of the proposed linear algorithm is shown in Figure 2.

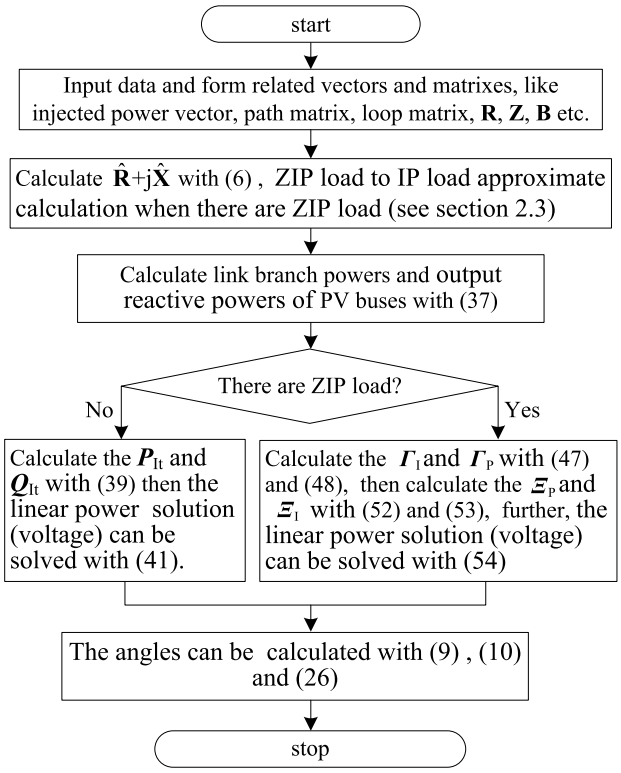

FIGURE 2. The flow chart of the proposed LPF method.

IV. NUMERICAL TESTS

In order to test the efficiency and accuracy of the proposed LPF, several existing LPF methods were applied and compared with the proposed method. The multi-phase and single-phase hybrid unbalanced 13bus, 37bus, 123bus system [24] and 615bus test systems are adopted. The 615bus system consists of five 123bus test system but total load was halved, and the connection topology of 615bus is shown in Figure 3. All the four test feeders include unbalanced ZIP star and delta connection loads with the unbalanced line parameters. The 123bus and 615bus systems have five and twenty-five backup link branches (loops) respectively. All the algorithms are programmed and realized in MATLAB 2015a (LAPTOP is THINKPAD with Intel Core I3-3110 CPU and 4.00GB Ram).

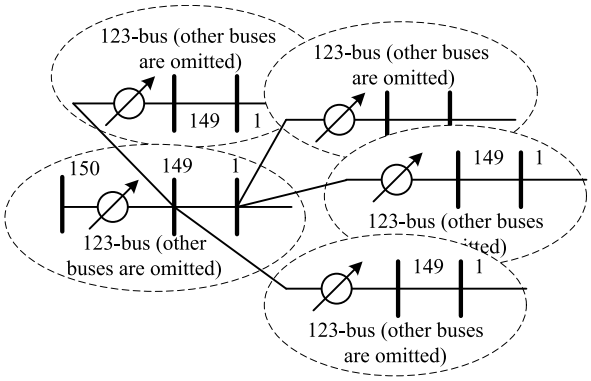

FIGURE 3. The connection topology of the improved 615-bus.

The results from the iterative loop-analysis based full AC power flow method (FACPF) in [23] and [25], are adopted as benchmarks (convergence accuracy is e-6 p.u.). Compared with the Newton-Raphson AC power flow methods and the backward / forward sweep power flow (BFS), FACPF can get the consistent results with the same precision but has much higher calculation efficiency especially for weakly-meshed networks [25].

The root-mean-squared (RMS) error of the voltage magnitude in (55), and the maximum absolute errors of the voltage magnitude and angle in (56)-(58) are used to investigate the performance of those LPFs.

$$\Delta U_{\mathrm{RMS}} = \sqrt{\sum_{i=1}^{\mathrm{N}} (U_{i\varphi} - \tilde{U}_{i\varphi})^2 / 3\mathrm{N}} (\varphi = a, b, c) \quad (55)$$

$$\Delta U_{\max} = \max(|U_{i\varphi} - \tilde{U}_{i\varphi}|, i = 1, ..., \mathrm{N}, \varphi = a, b, c) \quad (56)$$

$$\Delta \theta_{\max} = \max(|\theta_{i\varphi} - \tilde{\theta}_{i\varphi}|, i = 1, ..., \mathrm{N}, \varphi = a, b, c) \quad (57)$$

where, $U_{i\varphi}$ and $\theta_{i\varphi}$ denote the approximate values solved with the LPFs, $\tilde{U}_{i\varphi}$ and $\tilde{\theta}_{i\varphi}$ are the exact values solved with iterative loop-analysis method (FACPF).

The proposed LPF method is referred to LPLPF, other methods in this section consist of LALPF [13] (H.W. Li et al., 2019, a three-phase linear load flow solution based on loop-analysis theory), AGLPF [10] (Garces A., 2015, a Linear Three-Phase Load Flow for Power Distribution Systems), POLPF [18] (Wang Y et al., 2017, linear three-phase power flow for unbalanced active distribution networks with PV nodes). As discussed in Introduction, the LALPF and AGLPF are developed under rectangular coordinates and cannot deal with PV buses. POLPF and proposed LPLPF are developed under polar coordinates and can deal with PV buses. But the Delta connection loads are not discussed in POLPF.

A. NORMAL CONDITION

For the normal condition for four test systems, the relative results are listed in Table 1. Figure 4 shows the profiles of voltage magnitude for the radial 123bus test feeder with four LPFs and FACPF. In Table 1, the test feeder names including "Rd" denote the radial networks and the test feeder names including "Lp" denote the weakly meshed networks (the same below).

TABLE 1. Calculation results with different LPF methods for all test systems.

Method	item	13Rd	37 Rd	123 Rd	123Lp	615 Rd	615 Lp
	$U_{\min}$ (p.u.)	0.971	0.945	0.896	0.914	0.886	0.895
LALPF	$\Delta U_{\max}$(p.u.)	5.4e-5	5.7e-5	1.4e-3	7.0e-4	1.5e-3	1.1e-3
	ΔU_{RMS}(p.u.)	2.6e-5	2.8e-5	6.1e-4	3.4e-4	6.2e-4	4.9e-4
	$\Delta\theta_{\max}$ (°)	0.002	0.002	0.016	0.011	0.018	0.016
AGLPF	$\Delta U_{\max}$(p.u.)	5.4e-5	6.1e-5	1.4e-3	7.0e-4	1.5e-3	1.1e-3
	ΔU_{RMS}(p.u.)	2.7e-5	3.1e-5	6.1e-4	3.4e-4	6.3e-4	5.0e-4
	$\Delta\theta_{\max}$ (°)	0.002	0.002	0.016	0.011	0.018	0.017
POLPF	$\Delta U_{\max}$(p.u.)	1.2e-3	1.5e-2	1.3e-2	9.0e-3	1.5e-2	1.3e-2
	ΔU_{RMS}(p.u.)	6.7e-4	6.7e-3	6.4e-3	4.7e-3	7.4e-3	6.6e-3
	$\Delta\theta_{\max}$ (°)	0.076	0.654	0.664	0.448	0.790	0.661
LPLPF	$\Delta U_{\max}$(p.u.)	6.2e-4	6.3e-4	3.3e-3	2.7e-3	4.6e-3	4.2e-3
	ΔU_{RMS}(p.u.)	3.4e-4	4.2e-4	1.6e-3	1.7e-3	2.5e-3	2.6e-3
	$\Delta\theta_{\max}$ (°)	0.032	0.029	0.119	0.135	0.247	0.178

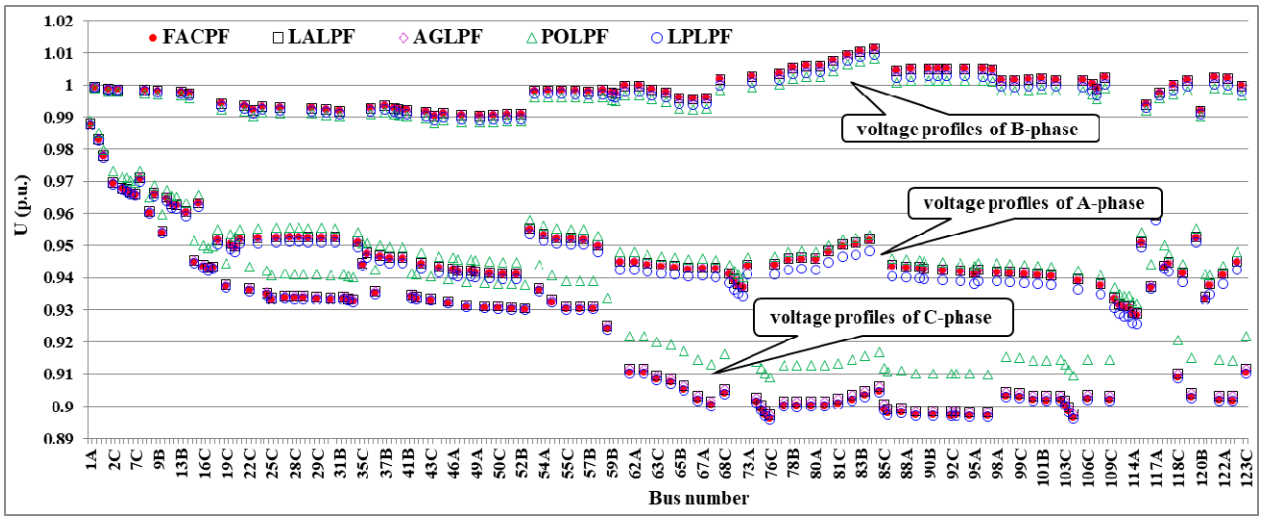

FIGURE 4. The profiles of voltage magnitude for radial 123bus test feeder.

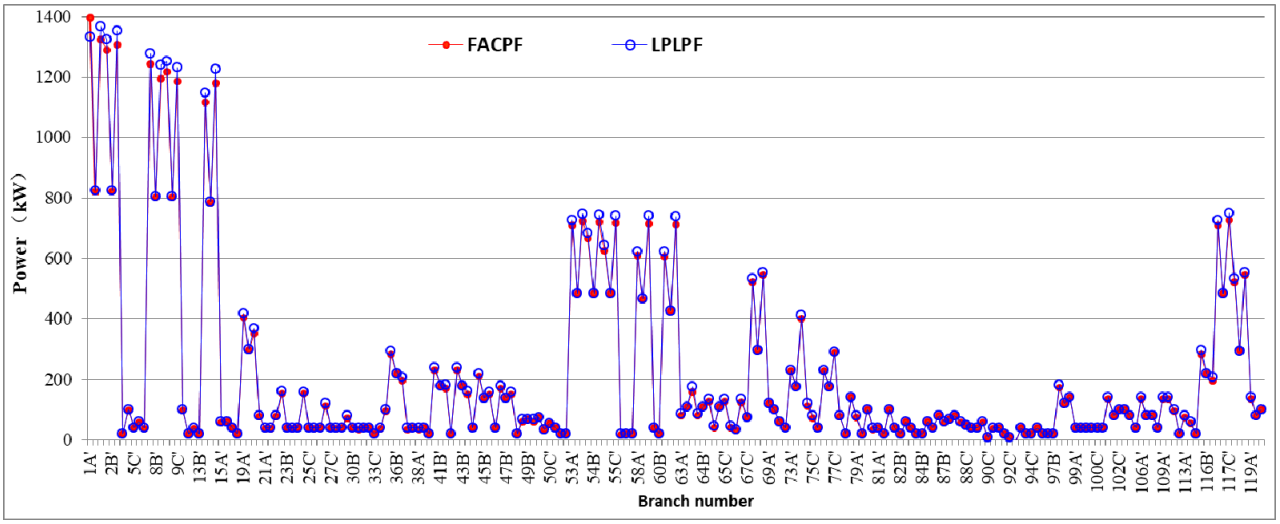

FIGURE 5. The branch kW flows for the radial IEEE 123bus test feeder.

It can be seen from Table 1 and Figure 4 (mark with the red solid circles are the exact values from FACPF), aiming at the accuracy, LALPF and AGLPF have almost the same results and perform the best. The reason is that the two linear methods adopt the same linearized approximations for ZIP loads. In addition, the line parameters of line model have not been approximated under rectangular coordinates for LALPF and AGLPF. The proposed LPLPF provides the much closer results with LALPF and AGLPF. The maximum magnitude errors are less than 0.01p.u for the solutions from those three LPFs (LALPF, AGLPF and the proposed LPLPF) even the minimum voltage magnitude is very low (it is only 0.886 p.u. for the radial 615bus system). But the errors with POLPF are relatively larger than other three methods. It can be seen from Figure 4, for the radial 123bus system, the voltage level of C-phase is the worst and the voltage level of B-phase is the best. It can be seen that there are obviously larger errors for POLPF when the voltage magnitudes are bad in C-phase.

Given that the operational voltage limit is typically between 0.95 and 1.05 p.u., the proposed LPLPF can be capable of offering an enough accuracy level even under a very heavily loaded system with bad voltage level. The proposed LPLPF has less precision than LALPF and AGLPF under rectangular coordinates if there are no PV buses, but LALPF and AGLPF can't deal with PV buses in the current models, so the proposed LPLPF is recommended when considering the high penetration of distributed renewable generation in DPS.

Moreover, with the proposed LPLPF, the three-phase branch reactive and active power flows can be obtained easily with (39), but other three LPFs do not derive the calculation formulations for the three-phase DPS. The benchmarks are also obtained with FACPF. Define the mean error and the root-mean-squared (RMS) error of the branch powers be,

$$\Delta P_{\text{MEAN}} = \frac{1}{3\text{N}} \sum_{i=1}^{\text{N}} (P_{i\varphi} - \tilde{P}_{i\varphi}) \Big/ \tilde{P}_{i\varphi}, \quad (\varphi = a, b, c) \tag{58}$$

$$\Delta P_{\text{RMS}} = \sqrt{\sum_{i=1}^{\text{N}} [(P_{i\varphi} - \tilde{P}_{i\varphi}) \Big/ \tilde{P}_{i\varphi}]^2 / 3\text{N}}, \quad (\varphi = a, b, c) \tag{59}$$

where, $P_{i\varphi}$ denotes the approximate value solved with the proposed LPLPF method and $\tilde{Pi\varphi}$ is the exact value solved with FACPF. The error results are listed in Table 2. It can be seen, the accuracy of the LPLPF in terms of kW flow is higher enough.

TABLE 2. The calculation errors of branch flows for the radial IEEE 123bus with proposed LPLPF.

Items	13Rd	37 Rd	123 Rd	123Lp	615 Rd	615 Lp
ΔP_{MEAN}	0.0113	0.0198	0.0222	0.0261	0.0330	0.0364
ΔP_{RMS}	0.0193	0.0326	0.0422	0.0482	0.0701	0.0727

Figure 5 presents the branch active power flow profiles of the radial 123bus test feeder with FACPF and LPLPF (the red solid circles are the benchmarks from FACPF and the blue hollow circles are the results from the proposed LPLPF). In Figure 5, the x-axis scale information means that the branches have been numbered with the terminal bus number of this branch by adding a single quote. It can be seen that the proposed LPLPF has a much high accuracy for almost all branches of the radial IEEE 123bus test system.

The calculation time has been presented in Table 3. The calculation time includes the coefficient matrix formation and power results solving for all LPFs. The results are the average value of 100 runs (the same below). Because the coefficient matrix dimension of the proposed LPLPF is half of the coefficient matrix dimension of other three LPFs, LPLPF has the fewest calculation time. FACPF needs to much more time for it needs iterative calculations. Moreover, because its coefficient matrix is a full matrix not the sparse matrix in other three LPFs, LALPF spent much more time than other LPFs for the large system [13].

TABLE 3. Computation time results with different LPF methods (s).

Method	13Rd	37 Rd	123 Rd	123Lp	615 Rd	615 Lp
FACPF	0.0028s	0.0078s	0.0405s	0.0353s	0.7640s	1.0200s
LALPF	0.0009s	0.0051s	0.0361s	0.0389s	1.6110s	1.9380s
AGLPF	0.0008s	0.0039s	0.0180s	0.0177s	0.7050s	0.6950s
POLPF	0.0007s	0.0041s	0.0224s	0.0221s	0.7890s	0.7770s
LPLPF	0.0005s	0.0033s	0.0143s	0.0159s	0.6210s	0.6250s

In addition, comparing Table 3 with Table 1 suggests that the proposed LPLPF obviously achieves a high computational efficiency with a bit worse calculation accuracy than LALPF and AGLPF. The LPLPF is therefore suitable for applications that require a large number of the iterative power flow calculations in DPS.

B. ILL CONDITION

To further validate the algorithm's ability to deal with ill-conditioned network, the radial 37bus test feeders under heavy load ratios are tested. The results are listed in Table 4 and the calculation time is shown in Figure 6.

TABLE 4. Calculation errors for 37bus in heavy ZIP loads with proposed LPLPF for all test systems.

Methods	item	Load ratio			
		100%	200%	300%	400%
	U_{min} (p.u.)	0.945	0.887	0.826	0.762
LALPF	ΔU_{max}(p.u.)	5.7e-5	5.0e-4	1.9e-3	5.1e-3
	ΔU_{RMS}(p.u.)	2.8e-5	2.5e-4	9.3e-4	2.5e-3
	$\Delta\theta_{max}$ (°)	0.002	0.019	0.073	0.207
AGLPF	ΔU_{max}(p.u.)	6.1e-5	5.1e-4	1.9e-3	5.1e-3
	ΔU_{RMS}(p.u.)	3.1e-5	2.5e-4	9.3e-4	2.5e-3
	$\Delta\theta_{max}$ (°)	0.002	0.019	0.073	0.207
POLPF	ΔU_{max}(p.u.)	1.5e-2	3.2e-2	4.9e-2	6.7e-2
	ΔU_{RMS}(p.u.)	6.7e-3	1.3e-2	2.0e-2	2.8e-2
	$\Delta\theta_{max}$ (°)	0.654	1.22	1.66	2.07
LPLPF	ΔU_{max}(p.u.)	6.3e-4	2.7e-3	6.5e-3	1.2e-2
	ΔU_{RMS}(p.u.)	4.2e-4	1.8e-3	4.5e-3	6.8e-3
	$\Delta\theta_{max}$ (°)	0.029	0.132	0.337	0.698

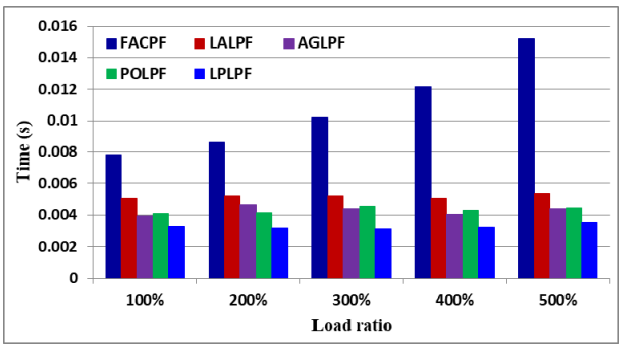

FIGURE 6. The histogram of calculation time with different methods in heavy ZIP load.

It can be seen from Table 4, when load ratio increases, the errors of voltage magnitude and phase angle increase obviously. But considering the bad voltage (even less than 0.7 p.u.), the accuracy is satisfactory for most practical applications in DPS with the proposed LPLPF as well as LALPF and AGLPF. The histograms of calculation time in Figure 6 show that the calculation time remains consistent during the heavy load conditions for all LPFs. This is one of the advantages of LPFs. Moreover, the proposed method has the fewest time than others for its 3N*3N coefficient matrix rather not the 6N*6N coefficient matrixes in other three LPFs. When load ratio increases, the iterative FACPF use more iterative calculations to meet the convergence accuracy. Thus, the higher the load ratio is, more time FACPF spends. Moreover, as discussed above, LALPF spends more time because of its full coefficient matrix.

V. CONCLUSION

The three-phase LPF solution is particularly important in the context of optimization operation and management of the modern DPS. So in this paper, several approximations have been derived first, and then a LPF model for unbalanced three-phase power distribution system has been developed based on the loop-analysis theory.

Compared with most other LPFs under rectangular coordinates or under polar coordinates, the proposed LPLPF has a 3N*3N coefficient matrix unlike other LPFs with the 6N*6N coefficient matrixes. So LPLPF has less calculation time than other LPFs.

Several standard power distribution systems with different load models and under heavy load ratio levels were tested. Results proved the effectiveness and accuracy of the proposed algorithm. The proposed LPLPF can provide a better accuracy and a higher calculation efficiency.

The proposed LPLPF provides a simpler, more robust, and potentially faster power flow solution for the three-phase unbalanced distribution networks. It can be effective to be applied in optimal load flow, economic power dispatch, contingency analysis, and reliability and security assessment of smart distribution system especially with the high penetration of distributed renewable generation into the system.

APPENDIX
DELTA CONNECTION LOAD TO STAR CONNECTION LOAD CONVERSION

For the proposed method can only handle the phase-ground loads (star connection load), so the delta connection load has to be specially dealt with. Considering that the three-phase voltage angles at the same bus are nearly symmetrical, that is, there are

$$\begin{cases} \dot{U}_{ab} = \dot{U}_a - \dot{U}_b \approx \sqrt{3}\dot{U}_a e^{j\frac{\pi}{6}} \\ \dot{U}_{bc} = \dot{U}_b - \dot{U}_c \approx \sqrt{3}\dot{U}_b e^{j\frac{\pi}{6}} \\ \dot{U}_{ca} = \dot{U}_c - \dot{U}_a \approx \sqrt{3}\dot{U}_c e^{j\frac{\pi}{6}} \end{cases} \quad (A.1)$$

Define the line **P** type load (delta connection load) vector as$P_L = [P_{ab}; P_{bc}; P_{ca}]$ and $Q_L = [Q_{ab}; Q_{bc}; Q_{ca}]$ at the terminal bus. Then reconsidering (5), the following equations can be derived for a delta connection load (herein, to simplify the derivation, the injected reactive powers from shunt **B** were

ignored).

$$\begin{aligned}
&\begin{bmatrix} U_{\mathrm{ia}}\angle\theta_{\mathrm{a}} \\ U_{\mathrm{ib}}\angle\theta_{\mathrm{b}} \\ U_{\mathrm{ic}}\angle\theta_{\mathrm{c}} \end{bmatrix} - \begin{bmatrix} U_{\mathrm{oa}} \\ U_{\mathrm{ob}} \\ U_{\mathrm{oc}} \end{bmatrix} \\
&= \boldsymbol{\Phi}^{-1}(\mathbf{R}+\mathrm{j}\mathbf{X})\mathbf{M}\begin{bmatrix} ((P_{\mathrm{ab}}+\mathrm{j}Q_{\mathrm{ab}})/\dot{U}_{\mathrm{ab}})^* \\ ((P_{\mathrm{bc}}+\mathrm{j}Q_{\mathrm{bc}})/\dot{U}_{\mathrm{bc}})^* \\ ((P_{\mathrm{ca}}+\mathrm{j}Q_{\mathrm{ca}})/\dot{U}_{\mathrm{ca}})^* \end{bmatrix} \\
&\approx (\hat{\mathbf{R}}+\mathrm{j}\hat{\mathbf{X}})\boldsymbol{\Phi}^{-1}\frac{e^{j\frac{\pi}{6}}}{\sqrt{3}}\mathbf{M}\boldsymbol{\Phi}\begin{bmatrix} (P_{\mathrm{ab}}-\mathrm{j}Q_{\mathrm{ab}})/U_{\mathrm{oa}} \\ (P_{\mathrm{bc}}-\mathrm{j}Q_{\mathrm{bc}})/U_{\mathrm{ob}} \\ (P_{\mathrm{ca}}\text{-}\mathrm{j}Q_{\mathrm{ca}})/U_{\mathrm{oc}} \end{bmatrix} \\
&\approx (\hat{\mathbf{R}}+\mathrm{j}\hat{\mathbf{X}})\mathrm{diag}\left(\frac{e^{j\frac{\pi}{6}}}{\sqrt{3}}\begin{bmatrix} 1 & 0 & -\alpha \\ -\alpha & 1 & 0 \\ 0 & -\alpha & 1 \end{bmatrix}\begin{bmatrix} P_{\mathrm{ab}}-\mathrm{j}Q_{\mathrm{ab}} \\ P_{\mathrm{bc}}-\mathrm{j}Q_{\mathrm{bc}} \\ P_{\mathrm{ca}}-\mathrm{j}Q_{\mathrm{ca}} \end{bmatrix}\right) \\
&\quad\times\begin{bmatrix} 1/U_{\mathrm{oa}} \\ 1/U_{\mathrm{ob}} \\ 1/U_{\mathrm{oc}} \end{bmatrix}
\end{aligned} \tag{A.2}$$

By comparing (A.2) with (5), the equivalent star connection load, $\hat{\boldsymbol{P}} = [\hat{P}_{\mathrm{a}};\hat{P}_{\mathrm{b}};\hat{P}_{\mathrm{c}}]$ and $\hat{\boldsymbol{Q}} = [\hat{Q}_{\mathrm{a}};\hat{Q}_{\mathrm{b}};\hat{Q}_{\mathrm{c}}]$, corresponding to the delta connection load can be obtained as following,

$$\begin{aligned}
\hat{\boldsymbol{P}}-\mathrm{j}\hat{\boldsymbol{Q}} &\approx \frac{e^{j\frac{\pi}{6}}}{\sqrt{3}}\begin{bmatrix} 1 & 0 & -\alpha \\ -\alpha & 1 & 0 \\ 0 & -\alpha & 1 \end{bmatrix}(\boldsymbol{P}_{\mathrm{L}}-\mathrm{j}\boldsymbol{Q}_{\mathrm{L}}) \\
&= \frac{(\sqrt{3}\mathbf{N}+\mathrm{j}\mathbf{M})(\boldsymbol{P}_{\mathrm{L}}-\mathrm{j}\boldsymbol{Q}_{\mathrm{L}})}{2\sqrt{3}}
\end{aligned} \tag{A.3}$$

Then (17) in section 2.3 can be obtained. And for a double-phase delta connection load, the relative equations can be derived similarly. Taking AB-phase for example,

$$\begin{cases}
\left[\hat{P}_{\mathrm{a}},\hat{P}_{\mathrm{b}}\right]^{\mathrm{T}} = \frac{1}{2}[1,-1]^{\mathrm{T}}P_{\mathrm{ab}} + \frac{1}{2\sqrt{3}}[1,1]^{\mathrm{T}}Q_{\mathrm{ab}} \\
\left[\hat{Q}_{\mathrm{a}},\hat{Q}_{\mathrm{b}}\right]^{\mathrm{T}} = \frac{1}{2}[1,-1]^{\mathrm{T}}Q_{\mathrm{ab}} - \frac{1}{2\sqrt{3}}[1,1]^{\mathrm{T}}P_{\mathrm{ab}}
\end{cases} \tag{A.4}$$

For **I** type delta connection load, redeveloping (A.3), it has,

$$\begin{aligned}
&\hat{\boldsymbol{P}}_{\mathrm{I}}-\mathrm{j}\hat{\boldsymbol{Q}}_{\mathrm{I}} \\
&= \frac{e^{j\frac{\pi}{6}}}{\sqrt{3}}\begin{bmatrix} 1,0,-\alpha \\ -\alpha,0,1 \\ 0,-\alpha,1 \end{bmatrix}\left(\vec{\boldsymbol{P}}_{\mathrm{L}}-\mathrm{j}\vec{\boldsymbol{Q}}_{\mathrm{L}}\right)\frac{1}{\sqrt{3}}\begin{bmatrix} U_{\mathrm{ab}} \\ U_{\mathrm{bc}} \\ U_{\mathrm{ca}} \end{bmatrix} \\
&\approx \frac{1}{3}\begin{bmatrix} 1,0,-\alpha \\ -\alpha,0,1 \\ 0,-\alpha,1 \end{bmatrix}\left(\vec{\boldsymbol{P}}_{\mathrm{L}}-\mathrm{j}\vec{\boldsymbol{Q}}_{\mathrm{L}}\right)\boldsymbol{\Phi}^{-1}\mathbf{M}^{\mathrm{T}}\boldsymbol{\Phi}U_{\mathrm{o}} \\
&= \frac{1}{12}\left(\sqrt{3}\mathbf{N}+\mathrm{j}\mathbf{M}\right)\left(\vec{\boldsymbol{P}}_{\mathrm{L}}-\mathrm{j}\vec{\boldsymbol{Q}}_{\mathrm{L}}\right)\left(\sqrt{3}\mathbf{N}^{\mathrm{T}}-\mathrm{j}\mathbf{M}^{\mathrm{T}}\right)\boldsymbol{U}_{\mathrm{o}}
\end{aligned} \tag{A.5}$$

Expanding (A.5) and rearranging them, then (20) can be derived. Similarly, for double-phase **I** type delta connection load, the relative equations can be derived similarly. Taking AB-phase for example,

$$\begin{cases}
\hat{\boldsymbol{P}}_{\mathrm{Iab}} \\
\approx \frac{1}{12}\left(\begin{array}{l} 3[1,1]^{\mathrm{T}}P_{\mathrm{ab}}[1,1] - \sqrt{3}[1,1]^{\mathrm{T}}Q_{\mathrm{ab}}[1,-1] \\ +[1,-1]^{\mathrm{T}}P_{\mathrm{ab}}[1,-1] + \sqrt{3}[1,-1]^{\mathrm{T}}Q_{\mathrm{ab}}[1,1] \end{array}\right) \\
\quad\times\begin{bmatrix} U_{\mathrm{oa}} \\ U_{\mathrm{ob}} \end{bmatrix} \\
\hat{\boldsymbol{Q}}_{\mathrm{Iab}} \\
\approx \frac{1}{12}\left(\begin{array}{l} 3[1,1]^{\mathrm{T}}Q_{\mathrm{ab}}[1,1] + \sqrt{3}[1,1]^{\mathrm{T}}P_{\mathrm{ab}}[1,-1] \\ +[1,-1]^{\mathrm{T}}Q_{\mathrm{ab}}[1,-1] - \sqrt{3}[1,-1]^{\mathrm{T}}P_{\mathrm{ab}}[1,1] \end{array}\right) \\
\quad\times\begin{bmatrix} U_{\mathrm{oa}} \\ U_{\mathrm{ob}} \end{bmatrix}
\end{cases} \tag{A.6}$$

Based on (11), it can deduce the following equations,

$$\begin{aligned}
\begin{bmatrix} U_{\mathrm{ab}}U_{\mathrm{ab}} \\ U_{\mathrm{bc}}U_{\mathrm{bc}} \\ U_{\mathrm{ca}}U_{\mathrm{ca}} \end{bmatrix} &= \mathrm{diag}\left(\begin{bmatrix} \dot{U}_{\mathrm{ab}} \\ \dot{U}_{\mathrm{bc}} \\ \dot{U}_{\mathrm{ca}} \end{bmatrix}\right)\begin{bmatrix} \dot{U}_{\mathrm{ab}} \\ \dot{U}_{\mathrm{bc}} \\ \dot{U}_{\mathrm{ca}} \end{bmatrix}^* \\
&\approx \begin{bmatrix} U_{\mathrm{oa}}U_{\mathrm{oa}}+U_{\mathrm{ob}}U_{\mathrm{ob}}+U_{\mathrm{oa}}U_{\mathrm{ob}} \\ U_{\mathrm{ob}}U_{\mathrm{ob}}+U_{\mathrm{oc}}U_{\mathrm{oc}}+U_{\mathrm{ob}}U_{\mathrm{oc}} \\ U_{\mathrm{oc}}U_{\mathrm{oc}}+U_{\mathrm{oa}}U_{\mathrm{oa}}+U_{\mathrm{oa}}U_{\mathrm{oc}} \end{bmatrix} \\
&\approx 3\begin{bmatrix} U_{\mathrm{oa}}+U_{\mathrm{ob}}-1 \\ U_{\mathrm{ob}}+U_{\mathrm{oc}}-1 \\ U_{\mathrm{oa}}+U_{\mathrm{oc}}-1 \end{bmatrix} = 3\left(\mathbf{N}^{\mathrm{T}}\boldsymbol{U}_{\mathrm{o}}-\boldsymbol{e}_3\right)
\end{aligned} \tag{A.7}$$

Then for **Z** type delta connection load, redeveloping (A.3) too, it has,

$$\begin{aligned}
&\hat{\boldsymbol{P}}_{\mathrm{Z}\varphi}-\mathrm{j}\hat{\boldsymbol{Q}}_{\mathrm{Z}\varphi} \\
&= \frac{e^{j\frac{\pi}{6}}}{\sqrt{3}}\begin{bmatrix} 1,0,-\alpha \\ -\alpha,0,1 \\ 0,-\alpha,1 \end{bmatrix}\left(\vec{\boldsymbol{P}}_{\mathrm{L}}-\mathrm{j}\vec{\boldsymbol{Q}}_{\mathrm{L}}\right)\frac{1}{3}\begin{bmatrix} U_{\mathrm{ab}}U_{\mathrm{ab}} \\ U_{\mathrm{bc}}U_{\mathrm{bc}} \\ U_{\mathrm{ca}}U_{\mathrm{ca}} \end{bmatrix} \\
&\approx \frac{1}{2}\left(\mathbf{N}+\mathrm{j}\frac{M}{\sqrt{3}}\right)\left(\vec{\boldsymbol{P}}_{\mathrm{L}}-\mathrm{j}\vec{\boldsymbol{Q}}_{\mathrm{L}}\right)\left(\mathbf{N}^{\mathrm{T}}\boldsymbol{U}_{\mathrm{o}}-\boldsymbol{e}_3\right)
\end{aligned} \tag{A.8}$$

Expanding (A.8) and rearranging them, then (22) can be derived. Similarly, for double-phase **Z** type delta connection load, the relative equations can be derived similarly. Taking AB-phase for example,

$$\begin{cases}
\hat{\boldsymbol{P}}_{\mathrm{Zab}} \\
\approx \frac{1}{2}\left([1,1]^{\mathrm{T}}P_{\mathrm{ab}}[1,1] + \frac{1}{\sqrt{3}}[1,-1]^{\mathrm{T}}Q_{\mathrm{ab}}[1,1]\right) \\
\times[U_{\mathrm{oa}},U_{\mathrm{ob}}]^{\mathrm{T}} - \frac{1}{2}\left([1,1]^{\mathrm{T}}P_{\mathrm{ab}} + \frac{1}{\sqrt{3}}[1,-1]^{\mathrm{T}}Q_{\mathrm{ab}}\right) \\
\hat{\boldsymbol{Q}}_{\mathrm{Zab}} \\
\approx \frac{1}{2}\left([1,1]^{\mathrm{T}}Q_{\mathrm{ab}}[1,1] - \frac{1}{\sqrt{3}}[1,-1]^{\mathrm{T}}P_{\mathrm{ab}}[1,1]\right) \\
\times[U_{\mathrm{oa}},U_{\mathrm{ob}}]^{\mathrm{T}} - \frac{1}{2}\left([1,1]^{\mathrm{T}}Q_{\mathrm{ab}} - \frac{1}{\sqrt{3}}[1,-1]^{\mathrm{T}}P_{\mathrm{ab}}\right)
\end{cases} \tag{A.9}$$

REFERENCES

[1] F. Dörfler and F. Bullo, "Novel insights into lossless AC and DC power flow," in *Proc. IEEE Power Energy Soc. Gen. Meeting*, Vancouver, BC, Canada, Jul. 2013, pp. 1–5.
[2] J. Zhang, X. Yao, B. Yin, and Y. He, "Fast solving method of ordered charging based on linearized equations of branch flow," *Dianli Xitong Zidonghua/Automat. Electr. Power Syst.*, vol. 42, no. 12, pp. 64–71, Jul. 2018.
[3] X. Rong, B. Wang, C. Shao, G. Yu, Y. Wang, Q. Sun, and Z. Bie, "Coordinated charging strategy of electric vehicle charging station based on combination of linear power flow and genetic algorithm," in *Proc. IEEE PES Asia–Pacific Power Energy Eng. Conf. (APPEEC)*, Xi'an, China, Oct. 2016, pp. 1772–1776.
[4] Z. Hu and X. Wang, "A probabilistic load flow method considering branch outages," *IEEE Trans. Power Syst.*, vol. 21, no. 2, pp. 507–514, May 2006.
[5] T. Ding, R. Bo, F. Li, Q. Guo, H. Sun, W. Gu, and G. Zhou, "Interval power flow analysis using linear relaxation and optimality-based bounds tightening (OBBT) methods," *IEEE Trans. Power Syst.*, vol. 30, no. 1, pp. 177–188, Jan. 2015.
[6] H. Ahmadi, J. R. Martí, and H. W. Dommel, "A framework for volt-VAR optimization in distribution systems," *IEEE Trans. Smart Grid*, vol. 6, no. 3, pp. 1473–1483, May 2015.
[7] H. Ahmadi and J. R. Martí, "Minimum-loss network reconfiguration: A minimum spanning tree problem," *Sustain. Energy Grids Netw.*, no. 1, pp. 1–9, Mar. 2015.
[8] L. Gan and S. H. Low, "Convex relaxations and linear approximation for optimal power flow in multiphase radial networks," in *Proc. Power Syst. Comput. Conf.*, Wroclaw, Poland, Aug. 2014, pp. 1–9.
[9] H. F. Zhai, Y. Wang, and M. Yang, "Linear approximation for power flow equation in multi phaseradial distribution network," *Adv. Technol. Elect. Eng. Energy*, vol. 36, no. 7, pp. 78–83, 2017.
[10] A. Garces, "A linear three-phase load flow for power distribution systems," *IEEE Trans. Power Syst.*, vol. 32, no. 1, pp. 827–828, Jan. 2015.
[11] J. R. Martí, H. Ahmadi, and L. Bashualdo, "Linear power-flow formulation based on a voltage-dependent load model," *IEEE Trans. Power Del.*, vol. 28, no. 3, pp. 1682–1690, Jul. 2013.
[12] H. Ahmadi, J. R. Martí, and A. von Meier, "A linear power flow formulation for three-phase distribution systems," *IEEE Trans. Power Syst.*, vol. 31, no. 6, pp. 5012–5021, Nov. 2016.
[13] H. W. Li, H. Zhu, and L. Pan, "A three-phase linear load flow solution based on loop-analysis theory for distribution system," *Int. J. Comput. Math. Elect. Electron. Eng.*, vol. 38, no. 2, pp. 703–723, Mar. 2019.
[14] A. J. G. Mena and J. A. M. Garcia, "An approximate power flow for distribution systems," *IEEE Latin America Trans.*, vol. 12, no. 8, pp. 1432–1440, Dec. 2014.
[15] P. Rossoni, W. Moreti da Rosa, and E. A. Belati, "Linearized AC load flow applied to analysis in electric power systems," *IEEE Latin Amer. Trans.*, vol. 14, no. 9, pp. 4048–4053, Sep. 2016.
[16] Z. Li, J. Yu, and Q. H. Wu, "Approximate linear power flow using logarithmic transform of voltage magnitudes with reactive power and power loss consideration," *IEEE Trans. Power Syst.*, vol. 33, no. 4, pp. 4593–4603, Jul. 2018.
[17] J. Yang, N. Zhang, C. Kang, and Q. Xia, "A state-independent linear power flow model with accurate estimation of voltage magnitude," *IEEE Trans. Power Syst.*, vol. 32, no. 5, pp. 3607–3617, Sep. 2017.
[18] Y. Wang, N. Zhang, H. Li, J. Yang, and C. Kang, "Linear three-phase power flow for unbalanced active distribution networks with PV nodes," *CSEE J. Power Energy Syst.*, vol. 3, no. 3, pp. 321–324, Sep. 2017.
[19] Y. Ju, C. Chen, L. Wu, and H. Liu, "General three-phase linear power flow for active distribution networks with good adaptability under a polar coordinate system," *IEEE Access*, vol. 6, pp. 34043–34050, 2018.
[20] H. Li, L. Pan, and Q. Liu, "A linear power flow solution for distribution power system including PV bus and ZIP load," *J. Elect. Eng. Technol.*, vol. 14, no. 5, pp. 1859–1870, Sep. 2019.
[21] H. Li, A. Zhang, X. Shen, and J. Xu, "A load flow method for weakly meshed distribution networks using powers as flow variables," *Int. J. Elect. Power Energy Syst.* vol. 58, pp. 291–299, Jun. 2014.
[22] H. Li, Y. Jin, A. Zhang, and X. Shen, "An improved hybrid load flow calculation algorithm for weakly-meshed power distribution system," *Int. J. Elect. Power Energy Syst.*, vol. 74, pp. 437–445, Jan. 2016.
[23] H. Li, H. Wu, and B. Jiang, "A three-phase hybrid power flow algorithm for meshed distribution system with transformer branches and PV nodes," *J. Elect. Eng. Technol.*, vol. 11, no. 1, pp. 65–75, 2016.
[24] *IEEE PES Distribution Systems Analysis Subcommittee Radial Test Feeders [EB/OL]*. Accessed: Sep. 23, 2018. [Online]. Available: http://sites.ieee.org /pes-testfeeders /resources/
[25] W. C. Wu and B. M. Zhang, "A three-phase power flow algorithm for distribution system power flow based on loop-analysis method," *Int. J. Elect. Power Energy Syst.*, vol. 30, no. 1, pp. 8–15, Jan. 2008.

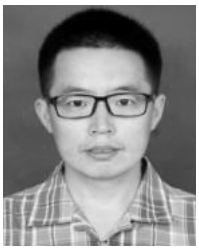

HONGWEI LI received the M.S. degree in electrical engineering from Southwest Jiaotong University, Chengdu, China, in 2005.

He is currently a Professor with Southwest Petroleum University (SWPU). His research interests include power system operation, multienergy management and optimization, renewable energy, and the integration of distributed generations into the grid.

HAILIN ZHOU received the B.S. degree in electrical engineering from Southwest Petroleum University (SWPU), Chengdu, China, in 2018, where he is currently pursuing the master's degree in control science and engineering.

His research interest includes microgrid modelling and control.

TONG LIU received the B.S. degree in electrical engineering from Southwest Petroleum University (SWPU), Chengdu, China, in 2019, where she is currently pursuing the master's degree in control science and engineering.

Her research interest includes power system analysis and control.

QI CHEN received the B.S. degree in electrical engineering from Southwest Petroleum University (SWPU), Chengdu, China, in 2018, where she is currently pursuing the master's degree in control science and engineering.

Her research interest includes microgrid optimization and control.